AD 612018

AFCRL-65-66

GDA-DBE64-067
Space Science Laboratory

THE FAR FIELD OF A ROCKET EXHAUST JET AT LOW AND MODERATE ALTITUDES

F. P. Boynton

General Dynamics/Astronautics
San Diego, California

ARPA Order No. 363
Contract No. AF 19(628)-4360
Project No. 8662

Scientific Report #1

December 1964

Prepared
for

AIR FORCE CAMBRIDGE RESEARCH LABORATORIES
OFFICE OF AEROSPACE RESEARCH
UNITED STATES AIR FORCE
BEDFORD, MASSACHUSETTS

GENERAL DYNAMICS | ASTRONAUTICS

Requests for additional copies by agencies of the Department of Defense, their contractors, or other government agencies should be directed to:

DEFENSE DOCUMENTATION CENTER (DDC)
CAMERON STATION
ALEXANDRIA, VIRGINIA 22314

Department of Defense contractors must be established for DDC services or have their "need-to-know" certified by the cognizant military agency of their project or contract.

All other persons and organizations should apply to the:

U.S. DEPARTMENT OF COMMERCE
OFFICE OF TECHNICAL SERVICES
WASHINGTON, D. C. 20230

Unclassified

Security Classification

DOCUMENT CONTROL DATA - R&D

(Security classification of title, body of abstract and indexing annotation must be entered when the overall report is classified)

1. ORIGINATING ACTIVITY *(Corporate author)* General Dynamics Corporation, Astronautics Division, San Diego, California	2a. REPORT SECURITY CLASSIFICATION Unclassified
	2b. GROUP

3. REPORT TITLE

The Far Field of a Rocket Exhaust Jet at Low and Moderate Altitudes

4. DESCRIPTIVE NOTES *(Type of report and inclusive dates)*

Scientific Report No. 1

5. AUTHOR(S) *(Last name, first name, initial)*

Boynton, Frederick P.

6. REPORT DATE December 1964	7a. TOTAL NO. OF PAGES 51	7b. NO. OF REFS 20
8a. CONTRACT OR GRANT NO. AF 19(628)-4360 ARPA Order No. 363	9a. ORIGINATOR'S REPORT NUMBER(S) GDA-DBE64-067	
b. PROJECT NO. 8662		
c. TASK	9b. OTHER REPORT NO(S) *(Any other numbers that may be assigned this report)* AFCRL-65-66	
d.		

10. AVAILABILITY/LIMITATION NOTICES Qualified requestors may obtain copies of this report from DDC. Other persons or organizations should apply to U.S. Department of Commerce, Office of Technical Services, Washington, D.C. 20230.

11. SUPPLEMENTARY NOTES	12. SPONSORING MILITARY ACTIVITY Air Force Cambridge Research Laboratories, CROO, United States Air Force, Bedford, Massachusetts

13. ABSTRACT

A method is given for predicting the flow field of a rocket exhaust plume at distances far removed from the nozzle exit at altitudes where afterburning of the exhaust is appreciable. The calculation combines a fluid mechanical analysis of turbulent mixing due to Libby with the adiabatic flame temperature calculation of Boynton and Neu. The eddy viscosity is determined from a consideration of conditions under which compressible turbulent flows appear to exhibit self-preserving behavior. Instructions are given for preparing input to two computer programs which are based on the analysis in this report. In two appendices, it is shown how the eddy viscosity constants may be derived from incompressible jet flow data and a comparison of the results of the present calculation with experimental wind-tunnel rocket exhaust behavior is given.

DD FORM 1473 1 JAN 64

Unclassified

Security Classification

Unclassified

Security Classification

14. KEY WORDS	LINK A ROLE	LINK A WT	LINK B ROLE	LINK B WT	LINK C ROLE	LINK C WT
Rocket exhaust Flow field Turbulent mixing Afterburning						

INSTRUCTIONS

1. ORIGINATING ACTIVITY: Enter the name and address of the contractor, subcontractor, grantee, Department of Defense activity or other organization *(corporate author)* issuing the report.

2*a*. REPORT SECURITY CLASSIFICATION: Enter the overall security classification of the report. Indicate whether "Restricted Data" is included. Marking is to be in accordance with appropriate security regulations.

2*b*. GROUP: Automatic downgrading is specified in DoD Directive 5200.10 and Armed Forces Industrial Manual. Enter the group number. Also, when applicable, show that optional markings have been used for Group 3 and Group 4 as authorized.

3. REPORT TITLE: Enter the complete report title in all capital letters. Titles in all cases should be unclassified. If a meaningful title cannot be selected without classification, show title classification in all capitals in parenthesis immediately following the title.

4. DESCRIPTIVE NOTES: If appropriate, enter the type of report, e.g., interim, progress, summary, annual, or final. Give the inclusive dates when a specific reporting period is covered.

5. AUTHOR(S): Enter the name(s) of author(s) as shown on or in the report. Enter last name, first name, middle initial. If military, show rank and branch of service. The name of the principal author is an absolute minimum requirement.

6. REPORT DATE: Enter the date of the report as day, month, year, or month, year. If more than one date appears on the report, use date of publication.

7*a*. TOTAL NUMBER OF PAGES: The total page count should follow normal pagination procedures, i.e., enter the number of pages containing information.

7*b*. NUMBER OF REFERENCES: Enter the total number of references cited in the report.

8*a*. CONTRACT OR GRANT NUMBER: If appropriate, enter the applicable number of the contract or grant under which the report was written.

8*b*, 8*c*, & 8*d*. PROJECT NUMBER: Enter the appropriate military department identification, such as project number, subproject number, system numbers, task number, etc.

9*a*. ORIGINATOR'S REPORT NUMBER(S): Enter the official report number by which the document will be identified and controlled by the originating activity. This number must be unique to this report.

9*b*. OTHER REPORT NUMBER(S): If the report has been assigned any other report numbers *(either by the originator or by the sponsor)*, also enter this number(s).

10. AVAILABILITY/LIMITATION NOTICES: Enter any limitations on further dissemination of the report, other than those imposed by security classification, using standard statements such as:

(1) "Qualified requesters may obtain copies of this report from DDC."

(2) "Foreign announcement and dissemination of this report by DDC is not authorized."

(3) "U. S. Government agencies may obtain copies of this report directly from DDC. Other qualified DDC users shall request through ________________."

(4) "U. S. military agencies may obtain copies of this report directly from DDC. Other qualified users shall request through ________________."

(5) "All distribution of this report is controlled. Qualified DDC users shall request through ________________."

If the report has been furnished to the Office of Technical Services, Department of Commerce, for sale to the public, indicate this fact and enter the price, if known.

11. SUPPLEMENTARY NOTES: Use for additional explanatory notes.

12. SPONSORING MILITARY ACTIVITY: Enter the name of the departmental project office or laboratory sponsoring *(paying for)* the research and development. Include address.

13. ABSTRACT: Enter an abstract giving a brief and factual summary of the document indicative of the report, even though it may also appear elsewhere in the body of the technical report. If additional space is required, a continuation sheet shall be attached.

It is highly desirable that the abstract of classified reports be unclassified. Each paragraph of the abstract shall end with an indication of the military security classification of the information in the paragraph, represented as *(TS)*, *(S)*, *(C)*, or *(U)*.

There is no limitation on the length of the abstract. However, the suggested length is from 150 to 225 words.

14. KEY WORDS: Key words are technically meaningful terms or short phrases that characterize a report and may be used as index entries for cataloging the report. Key words must be selected so that no security classification is required. Identifiers, such as equipment model designation, trade name, military project code name, geographic location, may be used as key words but will be followed by an indication of technical context. The assignment of links, rules, and weights is optional.

Unclassified

Security Classification

AFCRL-65-66

GDA-DBE64-067
Space Science Laboratory

THE FAR FIELD OF A ROCKET EXHAUST JET
AT LOW AND MODERATE ALTITUDES

F. P. Boynton

General Dynamics/Astronautics
San Diego 12, California

This work was sponsored by the Advanced
Research Projects Agency as a part of Project DEFENDER

ARPA Order No. 363
Contract No. AF 19(628)-4360
Project No. 8662

Scientific Report No. 1

December 1964

Prepared
for

AIR FORCE CAMBRIDGE RESEARCH LABORATORIES
OFFICE OF AEROSPACE RESEARCH
UNITED STATES AIR FORCE
BEDFORD, MASSACHUSETTS

TABLE OF CONTENTS

NOMENCLATURE

c_1	Parameter in eddy viscosity equation (upstream region)
c_2	Parameter in eddy viscosity equation (downstream region)
c_i	Mass fraction of ith species
h	Static enthalpy
J_i^T	Turbulent mass flux of ith species
ℓm	Reference length in self-preserving expressions
M	Mach number
$P*$	Reduced circular probability function
q^T	Turbulent heat flux
r	Radial coordinate
R	Transformed (Howarth) radial coordinate
u	Axial velocity component
v	Radial velocity component
x	Axial coordinate
ϵ	Turbulent exchange coefficient
η	Self-preserving radial coordinate
ξ	Transformed (Libby) axial coordinate
ρ	Density
ρ_o	Reference density
σ	Mach number correction to exchange coefficient
τ^T	Turbulent shear stress
ψ	Stream function; transformed (Libby) radial coordinate

Subscripts and superscripts

c	Denotes value along jet centerline
e	Denotes value in external stream
j	Denotes value at jet origin
1	Denotes difference between jet and freestream
*	Denotes quantity in transformed (Howarth) coordinates

THE FAR FIELD OF A ROCKET EXHAUST JET AT LOW AND MODERATE ALTITUDES

F. P. Boynton

ABSTRACT

A method is given for predicting the flow field of a rocket exhaust plume at distances far removed from the nozzle exit at altitudes where afterburning of the exhaust is appreciable. The calculation combines a fluid mechanical analysis of turbulent mixing due to Libby with the adiabatic flame temperature calculation of Boynton and Neu. The eddy viscosity is determined from a consideration of conditions under which compressible turbulent flows appear to exhibit self-preserving behavior. Instructions are given for preparing input to two computer programs which are based on the analysis in this report. In two appendices, it is shown how the eddy viscosity constants may be derived from incompressible jet flow data and a comparison of the results of the present calculation with experimental wind-tunnel rocket exhaust behavior is given.

INTRODUCTION

The flow far downstream from the nozzle exit of a rocket engine is governed primarily by viscous (turbulent) and chemical interactions with the surrounding atmosphere. The inviscid interactions caused by an initial imbalance between nozzle exit and ambient pressures have largely been dissipated in this region, and it is therefore appropriate to consider that these mixing and burning phenomena occur at relatively constant pressure. A description of this flow is then given by solving an initial-value problem for the boundary layer equations. The initial conditions are those of the rocket exhaust expanded to ambient pressure. For nozzle exit pressures close to ambient, the properties of this equivalent jet are given by an isentropic expansion of the exhaust. For nozzle exit pressures much greater than ambient, the non-isentropic analysis of Thomson[1] may be applied. For nozzle exit pressures much less than ambient (which are perhaps of lesser interest) the initial properties might be taken as those behind a normal shock at the jet exit.

In the following paragraphs we shall discuss briefly some elementary considerations of the structure of the far field which may be derived from a similarity analysis of jet flows in a coordinate system in which the boundary layer equation reduces to their incompressible form. We shall then discuss a linearized solution obtained by Libby,[2] and show how this analysis, combined with the considerations obtained from the similarity analysis, may be used to treat problems of rocket exhaust jets.

1. SIMILARITY CONSIDERATIONS

It is well known that the flow of a turbulent jet of constant-density fluid far from the origin is self-preserving: the variation of any mean quantity over any plane, x = constant, is expressible non-dimensionally through suitable scales of length and velocity, ℓ_m and u_m, as a universal function of y/ℓ_m. Analyses of the equations of motion for either the case where the jet velocity is much greater than that of the ambient medium or the case where the jet and ambient velocities differ by a small amount have shown that this behavior is possible, and a large number of experiments bear out that it really occurs.[3] However, the existence of full self-preservation in a jet flow with large density variations leads to an absurd result, that the density varies as a power of the axial distance. While this result is possible over a small region of the flow, its continuance violates the condition that the density must approach its free-stream value far downstream.

A transformation of the boundary layer equations exists which allows the coordinate system to be stretched or squeezed in such a manner as to eliminate the density as a variable. The equations then assume their incompressible form, and it is possible for self-preserving profiles to exist in the new coordinate system. The transformation is that of Howarth[4] and Dorodnitsyn,[5] wherein a new radial coordinate is introduced as

$$R = \left[\int_0^r 2\,\frac{\rho}{\rho_o}\,r'dr'\right]^{\frac{1}{2}} , \qquad (1)$$

where ρ_o is a suitably chosen reference value of the density. The boundary layer equations in terms of mean flow properties are these (for axially symmetric flow):

$$\left.\begin{aligned}
&\text{Continuity:}\quad \frac{\partial}{\partial x}(r\rho u) + \frac{\partial}{\partial r}(r\rho v) = 0\\
&\text{Momentum:}\quad \rho u\frac{\partial u}{\partial x} + \rho v\frac{\partial u}{\partial r} = -\frac{\partial P}{\partial x} + \frac{1}{r}\frac{\partial}{\partial r}\{r\tau^T_{xr}\}\\
&\text{Energy:}\quad \rho u\frac{\partial}{\partial x}[h+\frac{u^2}{2}] + \rho v\frac{\partial}{\partial r}[h+\frac{u^2}{2}] = \frac{1}{r}\frac{\partial}{\partial r}\{r(q^T_r+u\tau^T_{xr})\}\\
&\text{Species continuity:}\quad \rho u\frac{\partial c_i}{\partial x} + \rho v\frac{\partial c_i}{\partial r} = \frac{1}{r}\frac{\partial}{\partial r}\{rJ^T_{ri}\} + \overset{\circ}{w}_i
\end{aligned}\right] \tag{2}$$

The transformation $(x,r)\rightarrow(x,R)$ is performed by noting that

$$\frac{\partial}{\partial x} = \frac{\partial}{\partial x} + \frac{\partial R}{\partial x}\frac{\partial}{\partial R},\quad \frac{\partial}{\partial r} = \frac{\partial R}{\partial r}\frac{\partial}{\partial R} \tag{3}$$

and by requiring the stream function Ψ to be the same in each flow,

$$\Psi^* = \Psi. \tag{4}$$

By using the relations (3), and also noting that

$$u^* = \frac{1}{R}\frac{\partial\Psi}{\partial R},\quad v^* = -\frac{1}{R}\frac{\partial\Psi}{\partial x}, \tag{5}$$

whence

$$v^* = \frac{r}{R}\frac{\rho v}{\rho_o} + \frac{\partial R}{\partial x}u, \tag{6}$$

the following equations are obtained in place of the boundary layer equations:

$$\left.\begin{aligned}
&\text{Continuity:}\quad \frac{\partial u}{\partial x} + \frac{1}{R}\frac{\partial}{\partial R}(Rv^*) = 0\\
&\text{Momentum:}\quad u\frac{\partial u}{\partial x} + v^*\frac{\partial u}{\partial R} = \frac{1}{\rho_o R}\frac{\partial}{\partial R}(R\tau^{T*}_{xr})\\
&\text{Energy:}\quad u\frac{\partial}{\partial x}[h+\frac{u^2}{2}] + v^*\frac{\partial}{\partial x}[h+\frac{u^2}{2}] = \frac{1}{\rho_o R}\frac{\partial}{\partial R}\{R(q^{T*}_r + u\tau^{T*}_{xr})\}\\
&\text{Species continuity:}\quad u\frac{\partial c_i}{\partial x} + v^*\frac{\partial c_i}{\partial R} = \frac{1}{\rho_o R}\frac{\partial}{\partial R}\{RJ^{T*}_{ri}\}
\end{aligned}\right] \tag{7}$$

The reader will recognize that these are simply the boundary layer equations for an equivalent incompressible flow. The shear forces and flows of heat and matter are required to be the same for unit mass in both flows, whence

$$R\,\tau_{xr}^{T*}\,\rho_o\,dV^* = r\,\tau_{xr}^{T}\,\rho\,dV$$

$$R\,q_r^{T*}\,\rho_o\,dV^* = r\,q_r^{T}\,\rho\,dV$$

$$R\,J_{r,i}^{T*}\,\rho_o\,dV^* = r\,J_{r,i}^{T}\,\rho\,dV$$

where dV^* and dV are volume elements in the transformed and original coordinate systems.

We now wish to express the set of equations (7) in a self-preserving form. We can do this in two limiting cases, just as for incompressible flow. If we let u_e be the velocity of the external stream, and let u_1 be the difference between the local velocity in the jet and the free stream velocity, we may write the momentum equation as

$$(u_e + u_1)\,\frac{\partial u_1}{\partial x} + v^*\,\frac{\partial u_1}{\partial R} = \frac{1}{\rho_o R}\,\frac{\partial}{\partial R}\,\{R\,\tau_{xr}^{T*}\}\ . \tag{9}$$

We can either assume that $u_1 \gg u_e$ at every location of interest to us, or that $u_e \gg u_1$. These two cases will be investigated separately.

Case A ($u_1 \gg u_e$):

Here we choose the self-preserving functions $u_1 = u_m\,f(\eta)$, $v^* = u_m\,\zeta(\eta)$ and $\tau_{xr}^T = \rho_o\,u_m^2\,g(\eta)$, where $\eta = R/\ell_m$. We substitute these relations into equation (9) and perform a second coordinate transformation, $(x,r)\rightarrow(x,\eta)$. The result is

$$u_m\,\frac{du_m}{dx}\,f^2 - \frac{u_m^2}{\ell_m}\,\frac{d\ell_m}{dx}\,\eta f f' = \frac{u_m^2}{\ell_m}\left\{\frac{1}{\eta}\,(\eta g)' - \zeta f\right\} \tag{10}$$

The requirement for self-preservation is that the coefficients of the universal functions of η be either zero or proportional to each other. This requirement is satisfied if $\ell_m = \frac{1}{\sigma}\,(x-x_o)$ and $u_m \sim (x-x_o)^{-a}$, where σ is at most a function of the initial conditions and a is not yet determined. The momentum integral conservation equation is

$$2\pi \int_0^\infty \rho u_1^2 \, r dr = 2\rho_o \pi \int_0^\infty u_1^2 \, R dR = \pi u_m^2 \, \ell_m^2 \, \rho_o \left[2 \int_0^\infty f^2 \eta d\eta \right] = \pi r_j^2 \rho_j u_j \ , \tag{11}$$

which is obtained by letting the momentum flux across an axial station be that through the nozzle exit. The bracketed term is a constant, I_1, and we can set

$$u_1 = u_j \sqrt{\frac{\rho_j/\rho_o}{I_1}} \, \frac{r_j \sigma}{(x-x_o)} \, f(\eta) \tag{12}$$

This is the same relation (except for the presence of the term containing the nozzle and reference densities) as is obtained by Hinze for an incompressible flow. Thus $a = 1$, and $u_m \sim (x-x_o)^{-1}$.

The form of equation (12) suggests that the universal function $f(\eta)$ may be the same for compressible and incompressible jets. Data from several sources have been analyzed[6] to determine whether this congruency exists. It was found that for jets in which the Mach number was low, but where density variations were large, the profiles fell on the same curve when the reference density ρ_o was chosen to be ρ_e. Data from jets in which the initial Mach number was high gave curves which were narrower than the low-speed curve, but which could be brought into congruence with the low-speed curve by assuming that σ was a function of the initial Mach number. A choice which fit the data examined (which included only initially isoenergetic jets) quite well was $\sigma = \sqrt{1 + \frac{1}{2}(\gamma-1)M_j^2}$. This analysis indicated that the axial velocity decay of all jets in a stagnant ambient medium would be the same when plotted in an axial coordinate proportional to

$$\sqrt{\frac{\rho_e}{\rho_j}} \, \frac{(x-x_o)}{\sigma \, r_j} \ ,$$

and all jets examined followed this behavior. (We might note that this behavior was hypothesized by Thring and Newby[7] in a study of turbulent flames.)

To this point we have said nothing about the shape of the self-preserving functions $f(\eta)$, $\xi(\eta)$ and $g(\eta)$ except that they can be made the same for all jets. In order to proceed further, we require an assumption relating the shear stress to other parameters. Such a relation is obtained by introducing the concept of an eddy viscosity, ϵ_v, which is defined such that

$$\rho\epsilon_v \frac{\partial u}{\partial r} = \tau_{xr}^T \tag{13}$$

In many incompressible shear flows reasonable agreement of calculated and experimental velocity profiles are obtained by assuming ϵ_v is constant across any plane of constant x in the flow. The congruence of incompressible and (transformed) compressible velocity profiles suggests that a similar assumption could be applied to the compressible flow if the value of ϵ_v^* for the transformed coordinates is used. The values of ϵ_v^* and ϵ_v may be related to each other by remembering that the momentum flow per unit mass (i.e., the force exerted by shear stresses on a unit mass) is the same in the two systems. Thus

$$R\tau_{xr}^{T*} \rho_o RdRdxd\theta = r\tau_{xr}^T \rho rdrdxd\theta \tag{14}$$

or

$$\epsilon_v^* R^2 \rho_o{}^2 \frac{\partial u}{\partial R} dR = \epsilon_v r^2 \rho^2 \frac{\partial u}{\partial r} dr . \tag{15}$$

Now, since

$$\frac{\partial}{\partial r} = \frac{\partial R}{\partial r}\frac{\partial}{\partial r} ,$$

$$\frac{\partial u}{\partial r} = \frac{\partial R}{\partial r}\frac{\partial u}{\partial R} ,$$

and so

$$\epsilon_v = \epsilon_v^* \left(\frac{\rho_o R}{\rho r}\right)^2 \tag{16}$$

This representation of the eddy viscosity was first suggested in print by Ting and Libby.[8]

For actually calculating shear flows, we require an expression for ϵ_v^*. Since ϵ_v^* is defined as

$$\epsilon_v^* = \frac{\tau_{xr}^{T*}}{\rho_o \frac{\partial u}{\partial R}} \quad , \tag{17}$$

we may substitute the self-preserving function for τ_{xr}^{T*} and u, and express ϵ_v^* as

$$\epsilon_v^* = u_m \ \frac{(x-x_o)}{\sigma} \frac{g(\eta)}{f'(\eta)} \tag{18}$$

In order for ϵ_v^* to be constant for a given value of x, the ratio $g(\eta)/f'(\eta)$ must be a constant, K. If we identify u_m with u_c, the value of u on the centerline, and recognize that the transformed jet half-radius, $R_{\frac{1}{2}}$, is simply $\eta_{\frac{1}{2}}\ (x-x_o)$, we may express ϵ_v^* as

$$\epsilon_v^* = (K/\sigma\eta_{\frac{1}{2}})\ R_{\frac{1}{2}}\ u_c \ . \tag{19}$$

This is the form generally used for ϵ_v in incompressible jet flows* in a stagnant medium, with the exception of the "Mach number correction", σ.

If it is assumed that ϵ_v^* is constant across a plane of constant x, then Equation (10) may be solved for f. The result is

$$f(\eta) = [1+\frac{\eta^2}{8\alpha}]^{-2} \quad , \tag{20}$$

where $\alpha \sim \frac{\epsilon_v^*}{u_c x}$. This solution has been found to fit experimental radial velocity profiles in incompressible jets very well except in the outermost regions of the jet, where the calculated velocity drops off less rapidly than the measured velocity.

Case B ($u_e \gg u_1$):

Again we introduce the self-preserving functions $u_1 = u_m f(\eta)$, $v^* = u_m \zeta(\eta)$,

*Note that $R_{\frac{1}{2}}$ is proportional to a displacement thickness.

and $\tau_{xr}^{T*} = u_m^2 \rho_o g(\eta)$. The momentum equation becomes

$$u_e \left[\frac{du_m}{dx} f - \frac{u_m}{\ell m}\frac{d\ell_m}{dx}\eta f'\right] = \frac{u_m^2}{\ell m}\left[\frac{1}{\eta}(\eta g)'-\xi f'\right] \tag{21}$$

The integral equation of momentum conservation is

$$2\int_0^\infty \rho u_1(u_1+u_e)rdr = 2\int_0^\infty \rho_o u_1(u_1+u_e)RdR = 2\rho_o \ell_m^2 u_m u_e \int_0^\infty f\eta d\eta = u_e u_j \rho_j r_j^2 , \tag{22}$$

and the combination of (21) and (22) establishes that for self-preserving flow $\ell_m \sim (x+x_o)^{1/3}$, and $u_m \sim (x+x_o)^{-2/3}$. In this case we may express u_1 as

$$u_1 = \frac{u_j}{u_e}(u_j-u_e)\sqrt{\rho_j/\rho_e}\,\frac{1}{I_2}\left[\frac{\sigma r_j}{(x-x_o)}\right]^{2/3} f(\eta), \tag{23}$$

where we have again chosen ρ_e as the reference density.

If we introduce an eddy viscosity which is constant across a plane x = constant, then the equation for f may be solved to show

$$f = e^{-\frac{b}{2}\eta^2} \tag{24}$$

Again, it is possible to express ϵ_v^* as

$$\epsilon_v^* = (\text{const.}) \times (u_c R_{\frac{1}{2}}/\sigma) . \tag{25}$$

The Mach number correction factor, σ, seems to reflect a dependence on the partition of the total enthalpy of the jet into thermal and kinetic energy. In these terms, it might be more reasonable to speak of it as a Crocco number effect. The origin of this effect is not clear, but it may have to do with the production of sound by the turbulent jet. A recent review by Ribner[9] quotes results derived by Phillips,[10] who found an expression for the acoustic efficiency of a mixing layer at very high Mach numbers which may be expressed as

$$\eta = \frac{\text{acoustic energy flux}}{\rho U^3} = M^{-3/2} \frac{\overline{v^2}}{U^2} \frac{L^2}{\ell^2} .$$

Here 2U is the velocity difference between the streams, M is the Mach number, $\overline{v^2}$ is the mean square component of the fluctuating velocity normal to the flow direction, ℓ is a length scale of these fluctuations, and L is proportional to the thickness of the mixing zone. Ribner quotes experimental results on jet noise from rockets and aircraft engines which seem to indicate that the acoustic efficiency at high exhaust velocities is either independent of jet velocity or decreases slowly with increasing jet velocity.

In order to maintain a constant acoustic efficiency (in the context of Phillips' asymptotic expression) as the Mach number is increased, the ratio of the relative turbulent intensity v'/U to the relative scale ℓ/L must vary as $M^{3/4}$. The eddy diffusivity of a turbulent medium, on the other hand, may be written as $\epsilon \sim v'\ell$, or as the product of a (rms) fluctuating velocity and a scale. The asymptotic expression for σ suggested by the jet data is $\epsilon \sim M^{-1}$, and the variation of σ in the regime studied is more like $M^{3/4}$. This is compatible with Phillips' theory if v'/U remains more or less constant while ℓ/L decreases with increasing Mach number. This implies that the eddies are reduced in size, perhaps by the compressive action of shock waves, as the Mach number is increased. The whole field of turbulence at high Mach numbers remains quite speculative, and considerably more theoretical and experimental study is needed before any firm conclusions can be drawn. In the meantime, we must make do with the skimpy amount of data available. (The existing measurements of turbulence quantities in jets, such as those of Laurence, have only been made up to $M = 0.8$.)

2. LIBBY'S THEORY

Self-preserving flow is only found in the far field of jets when the ambient medium is essentially stagnant, or when the difference between jet and ambient velocities is small. In order to develop a method which could be extended to other parts of the jet and which can be used to treat flows where u_1 is neither much greater than u_e nor nearly equal to u_e, Libby obtained a linearized solution to the equations of motion of a jet. The momentum equation, with the shear stress expressed by Equation (13), is

$$\rho u \frac{\partial u}{\partial x} + \rho v \frac{\partial u}{\partial r} = \frac{1}{r} \frac{\partial}{\partial r} (\epsilon_v \rho_r \frac{\partial u}{\partial r}) \tag{26}$$

The procedures for obtaining the solution are slightly different when u_e is finite and when $u_e = 0$, but the solution for finite u_e reduces to that for $u_e = 0$ in the limit when transformed to the physical plane. We shall consider first Case B, u_e finite, and then Case A, $u_e = 0$. These correspond to the asymptotic cases $u_1 \ll u_e$ and $u_1 \gg u_e$ in the self-preserving solutions.

Case B ($u_e \neq 0$):

We apply the von Mises transformation to Equation (26), i.e., $(x,r) \rightarrow (x,\psi)$, where

$$\rho u r = \rho_e u_e \psi \frac{\partial \psi}{\partial r}, \quad \rho v r = - \rho_e u_e \psi \frac{\partial \psi}{\partial x}, \tag{27}$$

and obtain the result

$$\frac{\partial u}{\partial x} = \frac{1}{u_e \psi} \frac{\partial}{\partial \psi} \left[\epsilon \rho^2 r^2 u/\rho_e{}^2 u_e \psi^2) \psi \frac{\partial u}{\partial \psi} \right] , \tag{28}$$

where

$$r = \left[2 \int_0^{\psi} \frac{\rho_e u_e}{\rho u} \psi' d\psi' \right]^{\frac{1}{2}} \tag{29}$$

At this point we introduce the eddy viscosity in the Howarth-Dorodnitsyn coordinates,

$$\epsilon_v^* = \rho^2 r^2 \epsilon_v / \rho_o{}^2 R^2 \ ,$$

which may be shown to be

$$\epsilon_v^* = \rho^2 r^2 \epsilon_v / \rho_o \rho_e \ u_e \int_o^{\psi} \frac{2\psi' d\psi'}{u} \ . \tag{30}$$

Thus Equation (28) becomes

$$\frac{\partial u}{\partial x} = \frac{1}{u_e \psi} \frac{\partial}{\partial \psi} \left[\epsilon_v^* \left\{ \frac{u}{\psi^2} \int_o^{\psi} \frac{2\psi' d\psi'}{u} \right\} \psi \frac{\partial u}{\partial \psi} \right] . \tag{31}$$

If we now assume that ϵ_v^* is independent of r (and thus of ψ), and make the assumption that the term in curly brackets is identically one, we find that

$$\frac{\partial u}{\partial x} = \frac{\rho_o}{\rho_e} \frac{\epsilon_v^*(x)}{u_e \psi} \frac{\partial}{\partial \psi} [\psi \frac{\partial u}{\partial \psi}] \tag{32}$$

The assumption regarding the integral is essentially a linearization, for the bracketed term is really one only when $u - u_e \ll u_e$. We shall examine the effects of the linearization later.

We now transform the axial coordinate according to

$$\xi = \int_o^x \frac{\epsilon_v^*}{u_e \psi_j} \frac{\rho_o}{\rho_e} dx \ , \tag{33}$$

where

$$\psi_j = r_j \left(\frac{\rho_j u_j}{\rho_e u_e}\right)^{\frac{1}{2}} .$$

We then obtain the heat conduction equation,

$$\frac{\partial u}{\partial \xi} = \frac{\psi_j}{\psi} \frac{\partial}{\partial \psi} [\psi \frac{\partial u}{\partial \psi}] \ , \tag{34}$$

with the boundary conditions

$$u(0,\psi) = u_j \qquad (0 \le \psi \le \psi_j)$$

$$u(0,\psi) = u_e \qquad (\psi > \psi_j)$$

$$\lim_{\psi\to\infty} u(\xi,\psi) = u_e .$$

The solution to this problem is given by Carslaw and Jaeger[12] as

$$\frac{u-u_e}{u_j-u_e} = (1-e^{-\psi_j/4\xi})\, P^*\left(\frac{1}{\sqrt{2\xi/\psi_j}}, \frac{\psi/\psi_j}{\sqrt{2\xi/\psi_j}}\right) , \qquad (35)$$

where the function $P^*\ (\frac{Z}{\sigma}, \frac{R}{\sigma})$ has been tabulated by Masters.[13]

In order to transform to the physical plane, one must specify the density as a function of ψ and ϵ^* and perhaps ρ_o as a function of x. It was found from the similarity analysis that $\rho_o = \rho_e$ was a reasonable choice, since it allowed jets of varying density to be expressed by the same radial profiles. The expression for ϵ_v^* may be obtained by considering that in the upstream portion of the jet, the behavior is similar to that of a two-dimensional mixing layer, and in the downstream portion the behavior is that of a fully developed axially symmetric jet flow. Therefore, in the upstream region

$$\epsilon_v^* = c_1\ x(u_j-u_e)/\sigma \ , \qquad (36)$$

and in the downstream region

$$\epsilon_v^* = c_2\ R_{\frac{1}{2}}\ (u_c-u_e)/\sigma \qquad (37)$$

The transition point may be chosen to give good agreement with experiment.

Therefore, we may divide the transformation

$$x = \int_o^\xi \frac{u_e\psi_j}{\epsilon_v^*}\, d\ \xi'$$

into two parts. Above a certain value $\xi = \xi_o$, we have

$$\xi = \int_o^x \frac{c_1}{\sigma} \frac{u_j - u_e}{u_e} \frac{x'}{\psi_j} dx'$$

$$= \frac{\psi_j}{2} \frac{c_1}{\sigma} \frac{u_j - u_e}{u_e} \left(\frac{x}{\psi_j}\right)^2 ,$$

or

$$x = r_j \left[\frac{u_j}{u_j - u_e} \frac{\rho_j}{\rho_e} \frac{\sigma}{c_1} \frac{2\xi}{r_j}\right]^{\frac{1}{2}} \tag{38}$$

Beyond ξ_o, we have

$$x = x_o + \int_{\xi_o}^{\xi} \frac{\sigma u_e \psi_j d\xi'}{c_2 \, R_{\frac{1}{2}} (u_c - u_e)} \tag{39}$$

This relation may either be evaluated directly, or we may develop a somewhat more general relation which will allow changing c_2 and σ for a given computation more easily. By introducing the variable $S = 2\xi/\psi_j$, we can write (39) as

$$x = x_o + \frac{\psi_j}{2} \int_{S_o}^{S} \frac{\sigma u_e \psi_j dS'}{c_2 \, R_{\frac{1}{2}} (u_c - u_e)} \tag{40}$$

Recognizing that

$$u_c - u_e = (1 - e^{-1/2S}) \; (u_j - u_e)$$

and

$$R_{\frac{1}{2}} = \left[\int_o^{\psi_{\frac{1}{2}}} 2 \frac{u_e}{u} \psi' \; d\psi'\right]^{\frac{1}{2}}$$

(or, if $n = \psi/\psi_j$,

$$R_{\frac{1}{2}} = \psi_j \; [\int_o^{n_{\frac{1}{2}}(S)} 2 \frac{u_e}{u} n' dn']^{\frac{1}{2}}) \quad ,$$

we may write (40) as

$$x = x_o + \frac{\psi_j}{2} \int_o^S \frac{\sigma[u_e/(u_j-u_e)]\ dS'}{c_2(1-e^{-\frac{1}{2}S'})\ \left(\int_o^{n_{\frac{1}{2}}(S')} 2\ \frac{u_e}{u}\ n'\ dn'\right)^{\frac{1}{2}'}} . \qquad (41)$$

Now, from (35),

$$u = u_e + (u_j-u_e)(1-e^{-\frac{1}{2}S})\ P^*\ (S,n);$$

thus

$$x_o + \frac{\psi_j}{2} \int_o^S \frac{\sigma[u_e/(u_j-u_e)]^{\frac{1}{2}}\ dS'}{c_2(1-e^{-\frac{1}{2}S'})\ \left[\int_o^{n_{\frac{1}{2}}(S')} [(1-e^{-\frac{1}{2}S'})\ P^* + u_e/(u_j-u_e)]^{-1}\ 2n'\ dn'\right]^{\frac{1}{2}}} . \qquad (42)$$

Since $\psi_j = r_j(\frac{\rho_j u_j}{\rho_e u_e})^{\frac{1}{2}}$,

$$x = x_o + \frac{\sigma r_j}{2c_2} \left(\frac{u_j}{u_j-u_e}\right)^{\frac{1}{2}} \left(\frac{\rho_j}{\rho_e}\right)^{\frac{1}{2}} F(S_o, S, \frac{u_e}{u_j-u_e}) , \qquad (43)$$

where

$$F = \int_{S_o}^S \left[(1-e^{-\frac{1}{2}S'})^2 \int_o^{n_{\frac{1}{2}}(S')} \frac{2n'\ dn'}{(1-e^{-\frac{1}{2}S'})\ P^* + \frac{u_e}{u_j-u_e}} \right]^{-\frac{1}{2}} dS' .$$

The evaluation of the integral becomes somewhat easier far from the origin, where

$$1 - e^{-\frac{1}{2}S} \approx \frac{1}{2S}$$

and

$$P^*(S,n) \approx e^{-n^2/2S} \; .$$

Then

$$F = F(S_1) + \int_{S_1}^{S} \left[\left(\frac{1}{2S'}\right)^2 \int_0^{\sqrt{2S'\ell n2}} \frac{2n'dn'}{\frac{1}{2S'} e^{-n^2/2S'} + \frac{u_e}{u_j - u_e}} \right]^{-\frac{1}{2}} dS', \tag{44}$$

If we let $k = \frac{u_e}{u_j - u_e}$, the inner integral may be evaluated analytically to give

$$F = F(S_1) + \int_{S_1}^{S} \left[\frac{1}{2kS'} \left\{\ell n \frac{2k + \frac{1}{2S'}}{k + \frac{1}{2S'}}\right\}\right]^{-\frac{1}{2}} dS' \; . \tag{45}$$

The radial transform to the physical plane is given as

$$r = [2 \int_0^{\psi} \frac{\rho_e u_e}{\rho u} \psi' d\psi']^{\frac{1}{2}} \tag{46}$$

Because in an afterburning rocket exhaust the density is not a simple function of the velocity, this transform requires a greater knowledge of the details of the flow field. We shall discuss the requirements in a later section.

Case A ($u_e = 0$):

In this case we express the von Mises transform as

$$\rho u r = \rho_j u_j \; \psi \frac{\partial \psi}{\partial r}, \; \rho v r = - \rho_j u_j \; \psi \frac{\partial \psi}{\partial x} , \tag{47}$$

and the momentum equation becomes

$$\frac{\partial u}{\partial x} = \frac{1}{u_j\psi}\frac{\partial}{\partial\psi}\left[(\epsilon\rho^2 r^2 u/\rho_j^2 u_j \psi^2)\ \psi\ \frac{\partial u}{\partial\psi}\right] \tag{48}$$

With the same assumptions about the constancy of ϵ_v^* and the reference density ρ_o, and the same sort of linearization, (48) becomes

$$\frac{\partial u}{\partial x} = \frac{\rho_e}{\rho_j}\frac{\epsilon_v^*}{u_j\psi}\frac{\partial}{\partial\psi}\left[\psi\ \frac{\partial u}{\partial\psi}\right] . \tag{49}$$

By introducing a new axial coordinate

$$\xi = \int_o^x \left(\frac{\rho_j}{\rho_e}\right)^{-1} \frac{\epsilon_v^*}{u_j r_j}\, dx' , \tag{50}$$

the heat conduction equation is obtained as before,

$$\frac{\partial u}{\partial\xi} = \frac{r_j}{\psi}\frac{\partial}{\partial\psi}\left[\psi\ \frac{\partial u}{\partial\psi}\right] . \tag{51}$$

In this case the solution is

$$\frac{u}{u_j} = (1-e^{-r_j/4\xi})\ P^*\left(\frac{1}{\sqrt{2\xi/r_j}}, \frac{\psi/r_j}{\sqrt{2\xi/r_j}}\right) . \tag{52}$$

To transform the solution to the physical plane we again assume that in the upstream region of the jet

$$\epsilon_v^* = c_1\ x\ u_j/\sigma$$

and downstream

$$\epsilon_v^* = c_2\ R_{\frac{1}{2}}\ u_c/\sigma .$$

Then in the upstream region we obtain the solution

$$x = r_j \left[\frac{\rho_j}{\rho_e}\frac{2\xi}{r_j}\frac{\sigma}{c_1}\right]^{\frac{1}{2}} , \tag{53}$$

which may be recognized as the limiting case of Equation (38) as $u_e \to 0$.

In the downstream region we have

$$x = x_o + \int_{\xi_o}^{\xi} \frac{\rho_j}{\rho_e}\frac{\sigma u_j r_j d\xi'}{c_2 R_{\frac{1}{2}} u_c} . \tag{54}$$

Proceeding as before, we find that

$$x = x_o + \frac{\sigma r_j}{2c_2}\left(\frac{\rho_j}{\rho_e}\right)^{\frac{1}{2}} \int \frac{dS'}{\left[(1-e^{-\frac{1}{2}S'}) \int^{n_{\frac{1}{2}}(S)} \frac{2n' dn'}{P^*(S,n)}\right]} \tag{55}$$

It will be noted that (55) is the limiting case of (43) when $u_e \to 0$. Thus,

$$x = x_o + \frac{\sigma r_j}{2c_2}\left(\frac{\rho_j}{\rho_e}\right)^{\frac{1}{2}} F(S_o,S,0) . \tag{56}$$

Far from the origin, (56) may be shown to become

$$x = x_o + \frac{\sigma r_j}{2c_2}\left(\frac{\rho_j}{\rho_e}\right)^{\frac{1}{2}} [F(S_o,S_1,0) + S-S_1] , \tag{57}$$

which may be derived from (56) by introducing the limiting form of P^* or from (45) by taking the limit as $k \to 0$. The radial transform is performed as before.

3. DESCRIPTION OF FLOW CHEMISTRY

In a reacting turbulent flow, a complete description of the progress of chemical reactions would be very complex. The rate expressions describing mean reaction velocities become (like other expressions) averages over fluctuating quantities, and the proper method of taking this average so as to produce correct results has not been discovered. We therefore have essentially three alternatives: the reaction effects may be neglected; the reactions may be accounted for by using finite-rate expressions which are adjusted to give good agreement with experimental results; or the reactions may be assumed to proceed very rapidly so that a condition of local chemical equilibrium exists. The first alternative cannot account for the large energy release which occurs during afterburning of the exhaust gases. The second requires extensive experimental data covering many different conditions in order that the "phenomenological" expressions may be checked. The third has drawbacks of its own, which will be discussed below, but still seems the most reasonable procedure for a rocket exhaust at low altitude. It is this approach that is used here.

Even if reactions are very fast, it is strictly improper to employ mean-flow variables in the equilibrium expressions unless all the fluctuations about the mean values are small. However, one may hypothesize that some distance downstream from the primary reaction zone the heat released by combustion of a given element of fluid will have been spread by diffusive effects to neighboring elements, so that the mean density in the region considered is approximately that given by assuming that the fluid is locally "well-stirred". We therefore should expect that the local equilibrium solution described by conventional thermodynamic expressions in terms of mean flow variables represents an approximation which is increasingly good as one moves downstream, away from the region where exhaust gases and the atmosphere first meet.

We have treated the chemistry of the reacting plume after the "adiabatic flame temperature" approach proposed by Boynton and Neu.[14] Here the density, composition, velocity, and temperature may be expressed as functions of one variable, the mass fraction of exhaust gases in the local flow. The computation assumes local conservation of momentum, mass, and total enthalpy (including heats of formation) on mixing. This represents a solution of the set of equations (2) if the fluxes of mass and heat and the shear stresses are represented by equations of the form

$$\left.\begin{aligned} J_{r,i}{}^{T} &= \rho\epsilon_M \frac{\partial c_i}{\partial r} \\ q_{r,i}{}^{T} &= \rho\epsilon_H \frac{\partial T}{\partial r} \\ \tau_{x,r}{}^{T} &= \rho\epsilon_v \frac{\partial u}{\partial r} \end{aligned}\right] \qquad (78)$$

and if in addition $\epsilon_M = \epsilon_H = \epsilon_v$ everywhere in the flow field. Under these conditions, if the local mass fraction of fluid which originally came from the exhaust jet is c_j, then

$$\left.\begin{aligned} u &= c_j u_j + (1-c_j)\, u_e \;, \\ h + \tfrac{1}{2}u^2 &= c_j(h_j+\tfrac{1}{2}u_j^2) + (1-c_j)(h_e+\tfrac{1}{2}u_e^2) \;. \end{aligned}\right] \qquad (79)$$

The method of Boynton and Neu is to assume that u_j and h_j are determined by an isentropic expansion of the exhaust gases to ambient pressure. (This is not an essential feature of the computation, and a non-isentropic expansion - for example, by Thomson's method - may be employed if the nozzle exit and free stream pressures are greatly different.) For a given value of c_j, the values of u and h are computed from (79). From the thermodynamic properties of the various chemical constituents, the temperature of the mixture is found by a straightforward iterative procedure. At this point, no chemical reaction is assumed.

The effects of chemical reactions are considered in the following manner. A trial temperature is chosen, and from this temperature and the known pressure and atomic composition of the mixture the mole numbers (per mole of exhaust fluid) are calculated by the technique of free energy minimization.[15] This process is then iterated until the static enthalpy of the burned gas at the trial temperature is equal to the value of h calculated from (79). It is assumed that the energy release does not accelerate the flow, so that the velocity is the same regardless of whether the fluid has burned. This assumption is compatible with the coordinate transformations (1) and (27) in the above analysis of the momentum equation, where it is assumed that the only effect of a density change is a squeezing or stretching of the radial coordinate. Since

$$c_j = \frac{u-u_e}{u_j-u_e} , \tag{80}$$

this analysis can be combined directly with Libby's jet flow theory to provide a map of velocity, temperature, and composition throughout the flow field.

4. THE COMPUTER PROGRAMS "SHARP" AND "SHEAR"

The analysis presented in the preceding sections has been embodied in two computer programs. The first program, "SHARP", computes the detailed composition and temperature at a given mixing ratio between two streams whose properties are known, using the techniques of the previous section. The second program, "SHEAR", uses the output data of "SHARP" to compute the flow field by an integral transformation of Libby's solution to the physical plane.

The program "SHARP" is built up of a number of subroutines, some of which were developed for earlier programs ("Polyphase Chemical Systems," which is a thermochemical calculation of equilibrium temperature and properties, and "PEEP," a propellant performance program) and some of which are specific to the afterburning problem. As a result, much of the input information required by SHARP is that used by PEEP. The following is a listing of the input needed for SHARP and prescriptions for obtaining it.

Card No. 1 (Field width 3): NDS - number of chemical species* in the mixed flow;

*A condensed phase is a different species for this purpose.

NT - number of temperatures in the thermodynamic property tables; NALT - the number of different altitudes to be considered; NCAIR - the number of atmospheric constituents (usually two, N_2 and O_2). One card.

Card Group No. 2 (Field width 14): The thermodynamic property tables, one set of NT cards per species. These contain: T - temperature, °K; S - entropy (third law value) in cal/gm. mole-°K; H - enthalpy, defined as the heat of formation at zero °K (heats of formation of the elements in their normally occurring states - e.g., H_2(g), C(s) - are taken as zero) plus the heat required to raise the species to temperature T, in cal/gm. mole; CP - heat capacity in cal/gm. mole-°K. Additional information, such as species identity, may be included at the right-hand side of the card. Cards for most species of general interest are available in the Space Science Laboratory. NT x NDS cards.

Card Group No. 3 (Field width 14): Atmospheric and trajectory properties, two cards for each altitude. First card contains: ALT - altitude; PALT - atmospheric pressure in atm.; VALT - missile velocity in ft/sec.; TALT - atmospheric temperature in °K. Second card contains mole fractions of atmospheric constituents, NCAIR entries. Atmospheric data is generally obtained from standard tables, velocity data from a trajectory. 2 x NALT cards.

Card Group No. 4 (Field width 3): IMR - number of mass ratios of air/jet gases to be considered; NDA - number of different atoms, or of some other ultimate components of the system; NDP - number of different phases in the system. One card.

Card Group No. 5 (Field width 14): TINC - lowest temperature in thermodynamic property tables; TOE - initial guess to temperature of expanded gases; TOB - initial guess to temperature of burned gases; HO - enthalpy of the system at some reference state (generally chamber conditions) in cal/gm. (This may be obtained by taking the enthalpy of one mole of the rocket's fuel in cal/gm. mole, adding to it the enthalpy of as many moles of oxidizer as are required by the mixture ratio at which the rocket is operated, and dividing by the mass of the fuel/oxidizer system in atomic weight units.); VO - velocity of the system at some reference state in ft/sec. (zero if chamber or reservoir conditions are chosen). One card.

Card Group No. 6 (Field width 14): FMR - the mass ratios of air to jet gas to be considered. IMR numbers, placed 5/card.

Card Group No. 7 (Field width 14): FMJ - the atomic weights of the different atoms in the system. NDA numbers placed 5/card.

Card Group No. 8 (Field width 3): IPHASE - the identification of the phase in which a particular species belongs (the gas phase is always phase no. 1). NDS number, 20/card.

Card Group No. 9 (Field width 6): V - originally, molar volumes of condensed species; now replaced by zeros, NDS number, 10/card.

Card Group No. 10 (Field width 6): A - number of atoms of the jth kind in the ith molecule. (For example, $a_{H,H_2O} = 2$; $a_{O,H_2O} = 1$, etc.) NDS entries, 10/card, for each atom; start a new card when starting a new atom. NDA groups of NDS entries total.

Card Group No. 11 (Field width 14): ZIN - composition of jet gas in moles/mole of "fuel". Mole numbers of atmospheric constituents not present in the initial jet, or of species produced by the combustion process, must not be zero, but are set equal to a very small number. NDS numbers, 5/card.

Card Group No. 12 (Field width 14): FM - molecular weights of species. NDS numbers, 5/card.

Card Group No. 13 (Field width 6): VAR - identification of the species (N_2, H_2, etc.). NDS entries, 12/card.

Card Group No. 14 (May use whole card): NAME - identification of the run. One card.

Card Group No. 15 (Field width 14): TO - temperature (in °K) from which isentropic expansion to ambient pressure begins; PO - pressure (in atm) from which expansion begins. These may be chosen more or less arbitrarily (i.e., rocket chamber, throat, or exit conditions), but must be consistent with each other. One card.

Wherever entries occur which are associated with specific species, or specific atoms, the entries must always be made in the same order.

The output from SHARP consists of the following quantities: Altitude, atmospheric pressure PA and missile velocity, VA; temperature, TE; and velocity, VE of the jet gases expanded to ambient pressure; mixing ratio, R; temperatures of the unreacted (TJ) and equilibrium (TB) jet/air mixture and mixture velocity VJ; mole numbers of the species on mixing and after reaction. This information is repeated for each mixing ratio and each altitude.

The program "SHEAR" is the second version of a jet mixing program. An earlier version, developed for an application to a launch phase countermeasures study, contained a logical error which affected the axial coordinate. In addition, the program was quite inefficient because a constant step size was used. In the present version the step size of both the radial and axial transformation is controlled by means of a check against the properties of the solution in the (ξ,Ψ) plane and an interval specified by the user. This results in a variable spacing in the output.

The input required for SHEAR consists of the following information:

Card Group No. 1 (Format 2I12, 4E12.4, 1E8.2): NDS - number of species; NC - number of jet/air ratios tabulated; TEST - the value of the jet mass fraction at which the transition between the "upstream" and the "downstream" eddy viscosity model is made; TOL - the fractional amount by which the centerline mass fraction is diminished to define the axial step size $\Delta\xi$; PRINT - a number which is set negative for no printout of input, zero for printout of input except for P* tables, and positive for printout of all input; ENDR - the air mass fraction at which the radial transformation is terminated; ENDX - the centerline jet mass fraction at which the axial transformation is terminated. One card.

Card Group No. 2 (Field width 12): R_i - value of jet mass fraction; T_i - value of temperature for the particular value of R; Z_{ij} - values of species mole numbers (in any units, moles/mole of mixture, moles/mole of fuel, etc.) for the particular value of R, in consistent order. 6 numbers/card until all NDS species are accounted for, therefore N cards/value of R. Start a new card for the next value of R; NC x N cards total.

Card Group No. 3 (Field width 12): M - molecular weights of the species. NDS entries, 6/card.

Card Group No. 4 (Field width 12): P - ambient pressure; TP - temperature of jet; TE - temperature of air or free stream; A - radius of jet; UP - jet velocity; UE - air velocity; SIGMA - Mach number correction to eddy viscosity; C1 - upstream region eddy viscosity constant; C2 - downstream region eddy viscosity constant. Two cards. Any absolute units may be used for pressure and temperature, and any units for velocity and jet radius.

The SHEAR program also requires as input the values of the P* function. A tabulation versus $\alpha = \frac{1}{\sqrt{2\xi/\psi_j}}$ and $\beta = (1-\psi/\psi_j)/\sqrt{2\xi/\psi_j}$ has been prepared from the data given by Masters and stored on tape 5274. This tape is available in the Digital Computer Laboratory.

The output of SHEAR consists of the following items: N, the index of the radial step (N=1 is always the centerline); X, the axial coordinate in the same units used for A; R, the radial coordinate in the same units used for A; T, the local temperature; U, the local velocity; and the local composition in mole fractions.

SHEAR also produces punched card output consisting of X, R, T, U, and the mole fractions of the first four species. This information is presented in a 8E10.4 format. These cards may be used as input to any calculations to be made using the flow field data. One computer run produces about 700 cards, depending on the tolerance used.

The operating time of these programs is apparently quite fast. SHARP load times average 5 millihours on the 7094; execution time for 12 mixing ratios of an RP-1 jet with the atmosphere at one altitude is 7 millihours. The corresponding SHEAR run had an execution time of 32 millihours. It is therefore possible to solve a complete far-field exhaust flow problem in less than 50 millihours of machine time once the input data are known.

The analysis of the turbulent mixing problem is equally applicable to the turbulent axially symmetric wake. In the programming of SHEAR, the eddy viscosity was set proportional to the absolute magnitude of the velocity difference $u-u_e$, so that SHEAR may be used for a wake problem where u_j may represent, for example, conditions at the "neck".

5. SUMMARY

At this point it seems desirable to summarize the foregoing analysis and discussion. We are interested in describing the flow field of a rocket exhaust jet at low and moderate altitudes. The most important processes governing the flow are the turbulent mixing of the exhaust gases with the atmosphere and the combustion of the fuel-rich exhaust. The method of analysis follows closely the analysis of Libby developed for the supersonic combustion of hydrogen. The value of the eddy viscosity appropriate to a jet flow is derived from an analysis of the conditions under which compressible jets exhibit self-preserving behavior. It is found that the spreading coefficient is independent of density when expressed in the proper coordinate system, but that an effect of Mach or Crocco number appears to be present. (It is shown that this effect can be related to the loss of turbulence energy as radiated sound.) A consistent development of Libby's theory is given, allowing smooth transitions between the case of zero and finite free-stream velocity. It is shown that the development of the turbulent jet depends on the density ratio ρ_j/ρ_e, the velocity defect ratio $(u_j-u_e)/u_e$, and the eddy viscosity constants c_1, c_2, and σ. The effects of reaction between the exhaust and the atmosphere are accounted for by assuming that the flow is locally well-stirred and in chemical equilibrium. Effective turbulent Prandtl and Schmidt numbers are assumed to be identically one. Under these assumptions the chemical problem may be decoupled from the hydrodynamical problem.

Two computer programs have been prepared which, when used together, solve the afterburning rocket exhaust flow problem for given initial conditions. Instructions are given for operating these programs. In the first appendix, the results of Libby's linearized theory are compared in detail with well-known self-preserving solutions and shown to be nearly equivalent. Values of the eddy viscosity constants c_1 and c_2 are derived from carefully obtained experimental data. In the second appendix, a comparison is made with the results of constant-density jet flow experiments and with rocket exhaust experiments conducted in a wind tunnel, and the agreement is shown to be satisfactory.

ACKNOWLEDGEMENT

The author wishes to thank Dr. Alex Thomson for his stimulating and helpful discussions. The computer program "SHARP" was prepared by Miss Sally Kline; the computer program "SHEAR II" was prepared by Mr. Robert Schapelle.

APPENDIX 1

COMPARISON OF SELF-PRESERVING AND LINEARIZED THEORY AND DETERMINATION OF c_2 AND c_1

The effects of the linearization on Libby's solution can be examined by comparing the predicted axial and radial velocity profiles with those developed in self-preserving (asymptotic) jet flows. Let us first consider Case A, $u_e = 0$. Along the axis,

$$u_c = u_j \left(1 - e^{-r_j/4\xi}\right) \tag{A-1}$$

or, as ξ becomes very large,

$$u_c \approx \frac{u_j r_j}{4\xi} . \tag{A-2}$$

Now from (57), we have $x = x_1 + \frac{\sigma r_j}{2c_2} \left(\frac{\rho_j}{\rho_e}\right)^{\frac{1}{2}} \frac{2\xi}{r_j}$, or

$$\xi = \frac{c_2}{\sigma} \left(\frac{\rho_e}{\rho_j}\right)^{\frac{1}{2}} (x - x_1) , \tag{A-3}$$

whence

$$u_c \approx u_j \frac{\sigma}{4c_2} \left(\frac{\rho_j}{\rho_e}\right)^{\frac{1}{2}} \frac{r_j}{x - x_1} \tag{A-4}$$

This is very nearly (12) for $f(\eta) = 1$; it is (12) exactly if $I_1^{\frac{1}{2}} = 4c_2$. From (20), we have

$$I_1 = \int_0^\infty 2\left[1 + \frac{\eta^2}{8\alpha}\right]^{-4} \eta d\eta$$

$$= \frac{8}{3} \alpha .$$

Then for exact correspondence between (61) and (12), we must have $c_2 = \sqrt{\frac{1}{6}\alpha}$.

The radial solution far downstream may be expressed (in the asymptotic limit of the P^* function) as

$$\frac{u}{u_c} = e^{-\psi^2/4\xi r_o}, \tag{A-5}$$

or, with the use of (61), as

$$\frac{u}{u_c} = e^{-\psi^2/4\,\frac{c_2}{\sigma}\left(\frac{\rho_e}{\rho_j}\right)^{\frac{1}{2}}(x-x_1)r_j} \tag{A-6}$$

The transformed (or equivalent incompressible) radial coordinate is expressed as

$$R^2 = 2\int_o^{\psi} \frac{\rho_j u_j}{\rho_e u}\,\psi'\,d\psi'$$

$$= \frac{\rho_j u_j}{\rho_e u_c}\int_o^{\psi^2} e^{(\psi^2)'/4\frac{c_2}{\sigma}\left(\frac{\rho_e}{\rho_j}\right)^{\frac{1}{2}}(x-x_1)r_j}\,d(\psi^2)' \tag{A-7}$$

With a little manipulation, (A-7) becomes

$$R^2 = \frac{16c_2^2}{\sigma^2}(x-x_1)^2\left[\frac{u_c}{u} - 1\right],$$

which may be rearranged to give

$$\frac{u}{u_c} = \left[1 + \frac{\eta^2}{16c_2^2}\right]^{-1}, \tag{A-8}$$

where $\eta = \sigma R/(x-x_1)$. In terms of α, (65) may be written

$$\frac{u}{u_c} = \left[1 + \frac{3\eta^2}{8\alpha}\right]^{-1} \tag{A-9}$$

The radial profiles obtained from (20) and from (A-9) are shown as functions of $\eta/2\sqrt{\alpha}$ in Figure 1. It is seen that the theory of Libby predicts profiles which are narrower than the self-preserving profiles near the center of the jet, and wider near the edge. Therefore, we should expect that properties of the flow which are very sensitive to the radial profiles, and particularly to the profiles at the edge of the jet, are somewhat inaccurately described by the linearized theory when $u_e = 0$. When u_e is finite, and particularly when $u_e \gg u_j - u_e$, Libby's theory should be as accurate as the similar solution, since here the similar solution is likewise linearized.

Here we have

$$x = x_1 + \frac{\sigma r_j}{2c_2} \left(\frac{u_j}{u_j - u_e}\right)^{\frac{1}{2}} \left(\frac{\rho_j}{\rho_e}\right)^{\frac{1}{2}} \int_{S_1}^{S} \frac{2kS' \, dS'}{\ell n\left\{\frac{2k + \frac{1}{2}S'}{k + \frac{1}{2}S'}\right\}} \qquad \text{(A-10)}$$

If $k \gg 1$ while $S' \ll 1$, then (A-10) becomes

$$x = x_2 + \frac{\sigma r_j}{2c_2} \left(\frac{u_j}{u_j - u_e}\right)^{\frac{1}{2}} \left(\frac{\rho_j}{\rho_e}\right)^{\frac{1}{2}} \left(\frac{2}{\ell n 2}\right)^{\frac{1}{2}} S^{3/2} \;, \qquad \text{(A-11)}$$

where the lower limit to the integral has been incorporated in x_2. Therefore

$$\frac{2\xi}{\psi_j} = \left(\frac{3c_2}{2/\ell n 2}\right)^{2/3} \frac{(u_j - u_e)^{2/3}}{(u_j - u_e)^{1/3}} \left(\frac{\rho_e}{\rho_j}\right)^{1/3} \left(\frac{x - x_2}{\sigma r_j}\right)^{2/3} \qquad \text{(A-12)}$$

and

$$\frac{u_c - u_e}{u_j - u_e} \approx \frac{1}{2} \left(\frac{2/\ell n^2}{3c_2}\right)^{2/3} \frac{(u_j - u_e)^{1/3}}{(u_j - u_e)^{2/3}} \left(\frac{\rho_j}{\rho_e}\right)^{1/3} \left(\frac{\sigma r_j}{x - x_2}\right)^{2/3} \qquad \text{(A-13)}$$

In this case, (A-13) reduces to the self-preserving expression (23) if

$$I_2 = 2\,\frac{(u_j-u_e)^{2/3}\,u_j^{2/3}}{u_e^{4/3}}\left(\frac{\rho_e}{\rho_j}\right)^{1/6}\left(\frac{3c_2}{2/\ell n2}\right)^{2/3} \tag{A-14}$$

Now consider the radial profile. In this case, in the far downstream region

$$\frac{u-u_e}{u_c-u_e} = e^{-\psi^2/4\xi\psi_j}\ , \tag{A-15}$$

and

$$R^2 = \int_0^{\psi} 2\,\frac{\rho_e u_e}{\rho_e u}\,\psi' d\psi'\ . \tag{A-16}$$

Upon substituting (A-15) into (A-16) and integrating, we obtain, after a bit of manipulation,

$$R^2 = 2\psi^2\ . \tag{A-17}$$

Therefore

$$\frac{u-u_e}{u_c-u_e} = e^{-R^2/2\xi\psi_j}\ , \tag{A-18}$$

and substituting for ξ from (A-12), we find

$$f(\eta) = \exp\left[-\eta^2/2(u_j-u_e)^{2/3}\,\frac{u_j^{2/3}}{u_e^{4/3}}\left(\frac{\rho_e}{\rho_j}\right)^{1/6}\left(\frac{3c_2}{2/\ell n2}\right)^{2/3}\right]\ , \tag{A-19}$$

where we have employed the relations

$$\psi_j = r_j\left(\frac{\rho_j u_j}{\rho_e u_e}\right)^{\frac{1}{2}}$$

$$\eta = \sigma R/R_j^{2/3}(x-x_o)^{1/3} \ ,$$

and

$$R_j = r_j(\rho_j/\rho_e)^{\frac{1}{2}} \ .$$

Then we have from (A-19) and the definition of I_2,

$$I_2 = 2\int_0^\infty f(\eta)\eta d\eta = 2\,\frac{(u_j-u_e)^{2/3}u_j^{\,2/3}}{u_e^{\,4/3}}\left(\frac{\rho_e}{\rho_j}\right)^{1/6}\left(\frac{3c_2}{2/\ln 2}\right)^{2/3} \ , \qquad \text{(A-20)}$$

which is in agreement with the requirement (A-14) for I_2 if Libby's solution and the similar solution are to give the same axial decay. Note also that (A-19) is of the same form as (24), and we have therefore defined the constant a in terms of known quantities.

Since we know the relation that must exist between c_2 and α, the constant appearing in (20), in order that Libby's analysis and the similarity analysis give the same axial velocity decay, we may determine c_2 from the many experiments which have been performed on fully developed incompressible jets. In Hinze's book, the value of α was given as 0.00196, from which

$$c_2 = \sqrt{\alpha/6} = 0.0177.$$

This value of c_2 assures the proper axial decay far downstream. It should be noted that this number is quite close to the factor relating ε, u, and the displacement thickness in the outer regions of a turbulent boundary layer.[16]

In the present case we have two slightly different values of $R_{\frac{1}{2}}$ in the self-preserving solution and in the linearized solution. Letting $y = \eta/\sqrt{4\alpha}$, we may solve (20) and (A-9) for $y_{\frac{1}{2}}$. The results are

$$y_{\frac{1}{2}} = 0.910$$

for the self-preserving expression (20), and

$$y_{\frac{1}{2}} = 0.816$$

for the linearized expression (A-9). Since

$$R_{\frac{1}{2}} = y_{\frac{1}{2}} \sqrt{4\alpha} \; (x-x_1)$$

$$= 2y_{\frac{1}{2}} \, c_2 \sqrt{6} \, (x-x_1),$$

where x_1 is the virtual origin of the jet, and since x is related to $S = 2\xi/\psi_j$ by (57), as

$$x-x_1 = \frac{R_j}{2c_2} S ,$$

we have

$$R_{\frac{1}{2}} = y_{\frac{1}{2}} \, S \sqrt{6} .$$

In order to give the correct value of ϵ_v^* at a given axial station, the value of $R_{\frac{1}{2}}$ derived from Libby's solution should be multiplied by 0.910/0.816, or 1.114. Therefore the effective value of c_2 is

$$c_2 = 0.0197$$

for the case of a stagnant ambient medium.

As an approximate interpolation formula between the two cases of $u_e = 0$ and $(u_j-u_e) \ll u_e$, we may use

$$c_2 = 0.0177 + 0.0020 \, e^{-k} ,$$

where $k = u_e/(u_j-u_e)$ and is zero when $u_e = 0$ and infinite when $u_j-u_e \to 0$. Use of this formula will give the proper velocity decay. Since the apparent turbulent Schmidt number found in incompressible flow is approximately 0.7, c_2 (and also c_1) should be multiplied by this value if composition decay is of interest. No really valid approximation exists for temperature decay in a system where viscous dissipation effects are large, but it might be expected to decay more like composition than velocity.

The behavior in the upstream portion of the jet is determined by the choice of c_1 and the value of ξ at which the transition is made between the two models for ϵ_v^*. The value of c_1 can be determined from experimental studies of mixing layer flows; here the solution for an incompressible flow is given by Schlichting as[17]

$$u = \tfrac{1}{2}(u_j+u_e)\{1- \frac{u_j-u_e}{u_j+u_e}\operatorname{erf}\,(\beta\,\frac{y}{x})\}\ , \qquad \text{(A-21)}$$

where $\beta = \frac{1}{2}\ (\frac{c_1}{\sigma}\,\frac{u_j-u_e}{u_j+u_e})^{-\frac{1}{2}}$ and $\frac{c_1}{\sigma}$ is defined as in (36).

The solution obtained by Libby, in the limit that $\frac{2\xi}{\psi_j}$ becomes very small, is given by

$$u = u_e + \tfrac{1}{2}\ (u_j-u_e)\ \left\{1-\operatorname{erf}\left[\frac{\psi/\psi_j\ -\ 1}{\sqrt{2}\ \sqrt{2\xi/\psi_j}}\right]\right\}\ . \qquad \text{(A-22)}$$

Evaluating the incompressible radius R, we find that when the linearization is valid $R \approx \psi$. Defining R_j as $\psi_j(u_e/u_j)$ or as $r_j\rho_j/\rho_e$, we may rewrite (A-22) as

$$u = u_e + \tfrac{1}{2}\ (u_j-u_e)\left\{1-\operatorname{erf}\left[\frac{R-R_j\,\frac{u_e}{u_j}}{R_j\,\frac{u_e}{u_j}}/\sqrt{2}\ \sqrt{2\xi/\psi_j}\right]\right\} \qquad \text{(A-23)}$$

Now we recognize that from (38)

$$\sqrt{2\xi/\psi_j} = \sqrt{\frac{c_1}{\sigma}\ \frac{u_j-u_e}{u_j}\ \frac{x}{R_j}}\ . \qquad \text{(A-24)}$$

Substituting this expression in (A-23), and assuming $u_e/u_j \simeq 1$, we obtain

$$u = u_e + \tfrac{1}{2}(u_j - u_e)\left\{1 - \mathrm{erf}\left[\frac{R-R_j}{x} \Big/ \sqrt{2\,\frac{c_1}{\sigma}\,\frac{u_j-u_e}{u_j}}\right]\right\}, \tag{A-25}$$

and by identifying y with $(R-R_j)$, noting that $u_j \approx \frac{1}{2}(u_j+u_e)$, and defining β as in Schlichting's solution, we find

$$u = u_e + \tfrac{1}{2}(u_j - u_e)\left\{1 - \mathrm{erf}(\beta \tfrac{y}{x})\right\} \tag{A-26}$$

This is exactly equivalent to (A-21), as may be seen by recognizing that

$$u_e = \tfrac{1}{2}\left[(u_j+u_e)-(u_j-u_e)\right] .$$

Since the solutions of Libby and Schlichting can here be made exactly equivalent,* the value of c_1 obtained from fitting mixing-layer experiments to the Schlichting solution can be used in transforming Libby's solution to the physical plane. Schlichting gives a value of $\beta = 13.5$ as the best fit to experimental data; Vasiliu selected a best value of 12.0. These values are for $u_e = 0$ at low jet Mach numbers, so that

$$c_1 = \frac{1}{4\beta^2} = 0.00174 .$$

The value of ξ_o can be determined either by numerical experiments, or by choosing it so that ϵ_v^* as given by the upstream expression is equal to ϵ_v^* as given by the downstream expression.

---

*Schlichting's solution is also linearized, since it represents the first two terms of a power series in $(u_j-u_e)/(u_j+u_e)$.

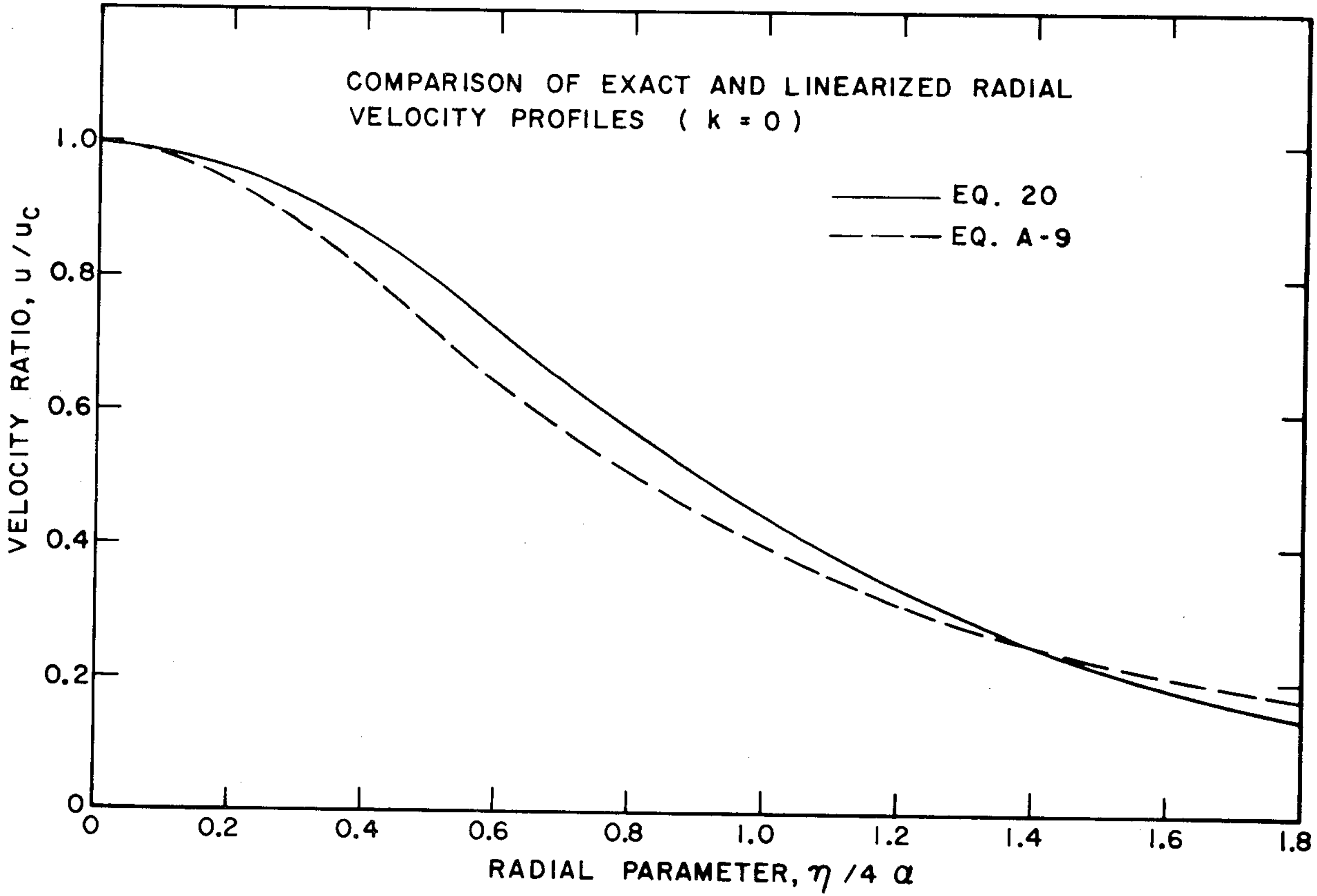

COMPARISON OF EXACT AND LINEARIZED RADIAL
VELOCITY PROFILES (k = 0)
EQ. 20
EQ. A-9
VELOCITY RATIO, u / u_c
RADIAL PARAMETER, $\eta / 4 \alpha$
1.0
0.8
0.6
0.4
0.2
0
0
0.2
0.4
0.6
0.8
1.0
1.2
1.4
1.6
1.8

Figure 1

APPENDIX 2

COMPARISON WITH EXPERIMENT

The analysis given in this report has been checked against experimental data presented by Corrsin and Uberoi,[18] by Forstall and Shapiro,[19] and in the final report of the Ballistic Missile Plume Wind-Tunnel Research Program.[20] The comparison with Corrsin and Uberoi is shown in Figure 2; except for a slight axial displacement, the agreement is excellent. (This result should have been expected, since the value of c_2 taken from the preceding section is taken from this experimental work.) The data given by Forstall and Shapiro show considerable experimental scatter. The results of a comparison with data from two different velocity ratios u_j/u_e are shown in Figures 3 and 4. The agreement appears to be fair, considering the scatter in the data.

Comparisons with data from actual rocket firings are difficult to obtain, since only a few data exist. The only source of data at altitude seems to be the wind-tunnel experiment performed by Convair in the AEDC facility. For a comparison here, we have chosen the results of the composition samplings. A comparison with the axial decay data at sea level may be found by plotting the reciprocal of the mass fraction of jet fluid versus axial distance. The self-preserving theory, and that of Libby in its asymptotic form, predict a linear relationship which should be the same for all jets when plotted versus an axial coordinate in units of equivalent jet radii, where

$$r_{equiv} = r_j \ (\rho_e/\rho_j)^{\frac{1}{2}}/\sigma \ .$$

The results of such a plot are shown in Figure 5, where a linear relation is shown to exist. We also show the reciprocal velocity decay of Corrsin and Uberoi, and the results of a "SHEAR II" run with the value of c_2 multiplied by 0.65, which is close to the value of the turbulent Schmidt number found in constant-density jets.[3] The agreement in slope between the computer calculation and the experiment is excellent. The experimental results show an apparent offset of the virtual origin of the flow. (This offset also appears in the runs at altitude, and may reflect an error in locating the sampling probe.)

Radial profiles calculated and measured are shown in Figure 6, where we have compared radial "slices" with nearly the same axial mass fraction for the experiment and the calculation. The agreement is again good, with the observed profiles slightly wider than the calculated ones because of the Schmidt number effect.

A comparison at altitude, where the free stream velocity is appreciable, has been made using the experimental results for the runs at 50,000 ft., with an external Mach number of 1.75. These data are from two different engines, one with an area ratio of 25/1 and the other with an area of 8/1, but with throat area, chamber pressure, and mixture ratio equal. The balanced jet assumption should apply to these data, and indeed the axial decay profiles shown in Figure 7 follow the same curve within the experimental errors. This decay curve can be fitted by the analysis, where σ is based on the velocity difference Mach number defined by the inner stream properties and an effective Schmidt number of 0.65 is employed. Since the apparent offset from the origin is found in these data also, we show only the region of the jet where the data were obtained. This is in the region of the largest volume of hot gas in an afterburning rocket exhaust, and the calculation is therefore suitable for use in a radiance prediction. The agreement of calculated and experimental radial profiles is shown in Figure 8, and appears to be as good as could be expected considering the scatter of the data.

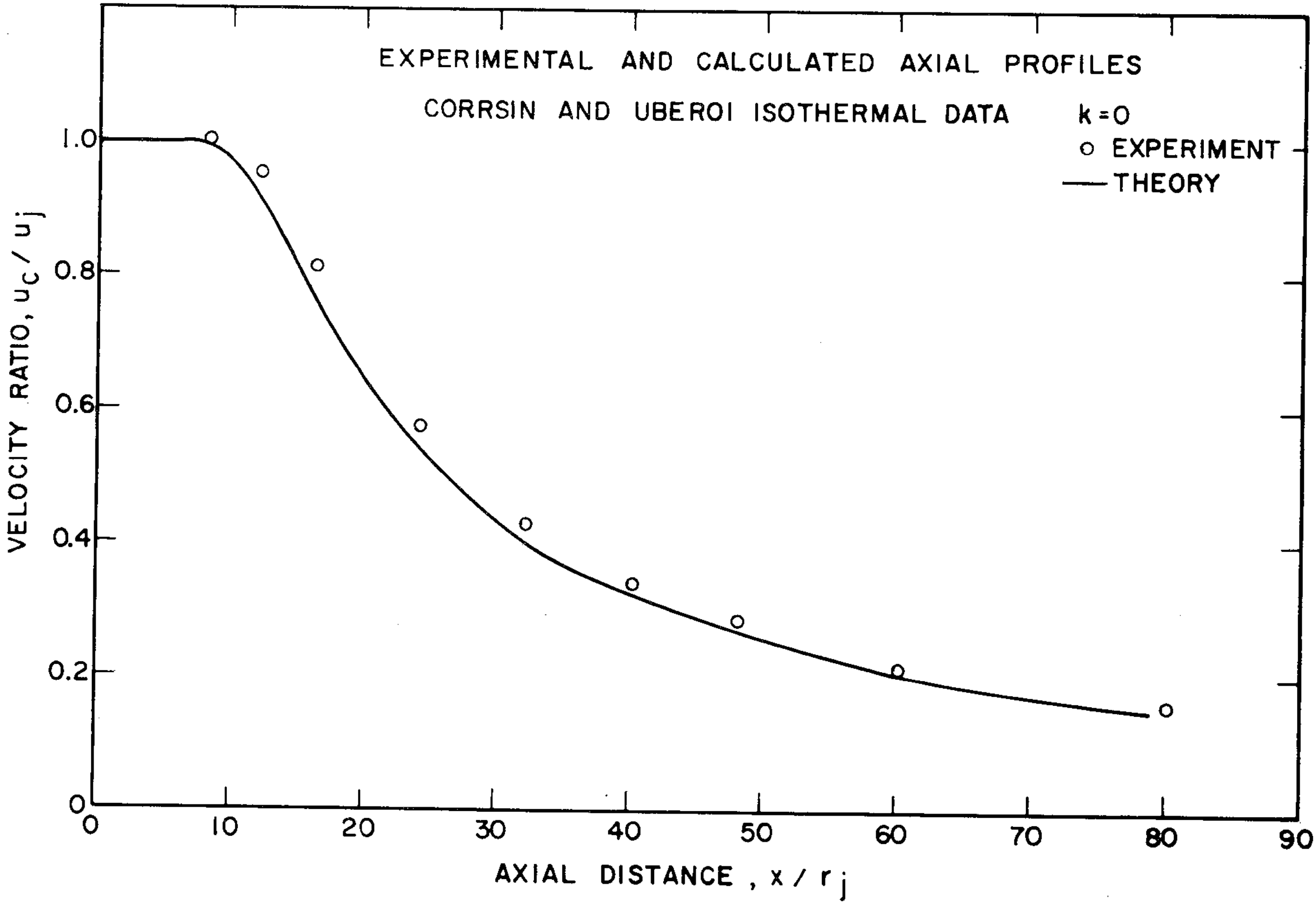
EXPERIMENTAL AND CALCULATED AXIAL PROFILES
CORRSIN AND UBEROI ISOTHERMAL DATA
k = 0
o EXPERIMENT
— THEORY
VELOCITY RATIO, u_c / u_j
1.0
0.8
0.6
0.4
0.2
0
10
20
30
40
50
60
70
80
90
AXIAL DISTANCE , x / r_j

Figure 2

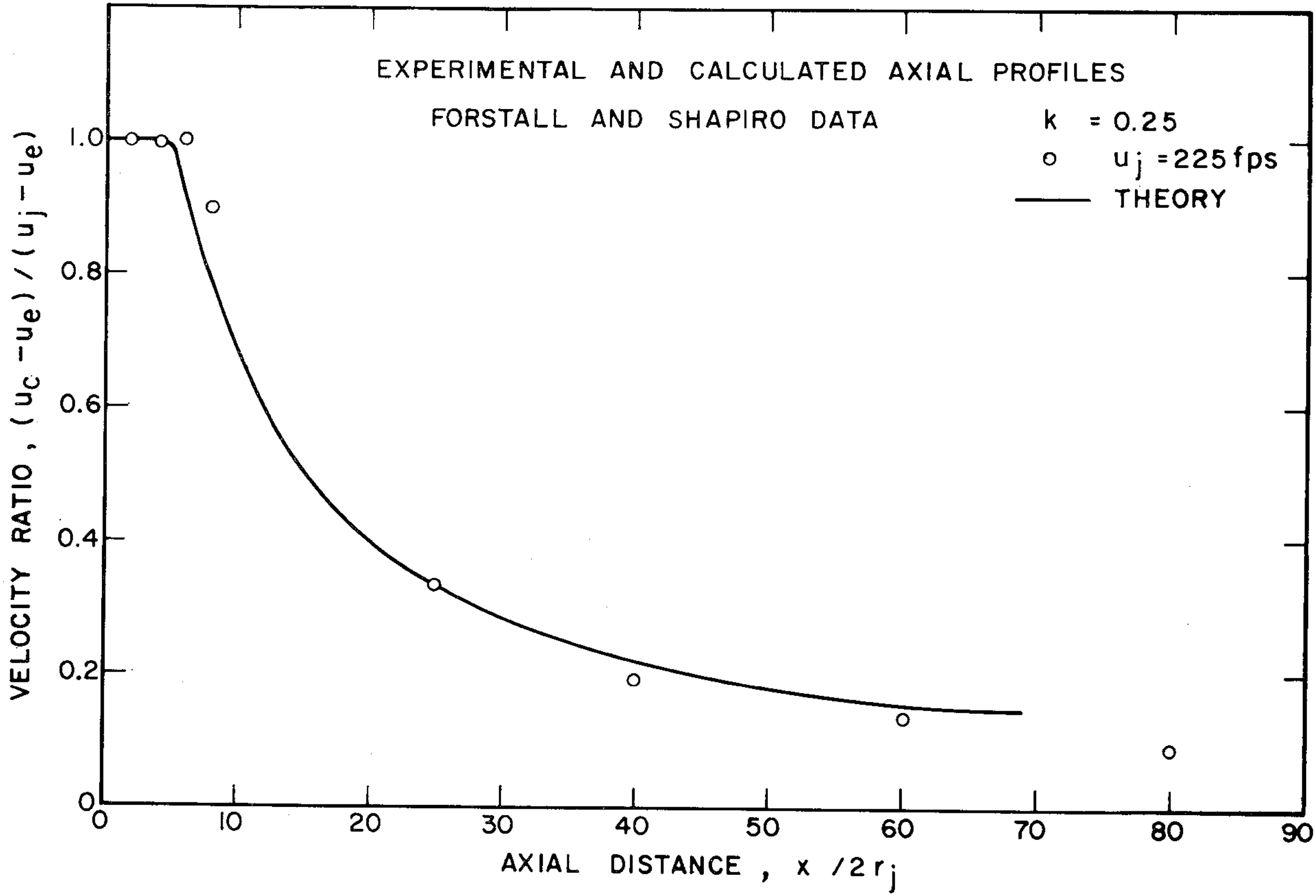
EXPERIMENTAL AND CALCULATED AXIAL PROFILES
FORSTALL AND SHAPIRO DATA
k = 0.25
u_j = 225 fps
THEORY
VELOCITY RATIO, $(u_c - u_e)/(u_j - u_e)$
AXIAL DISTANCE, $x/2r_j$
0
0.2
0.4
0.6
0.8
1.0
10
20
30
40
50
60
70
80
90

Figure 3

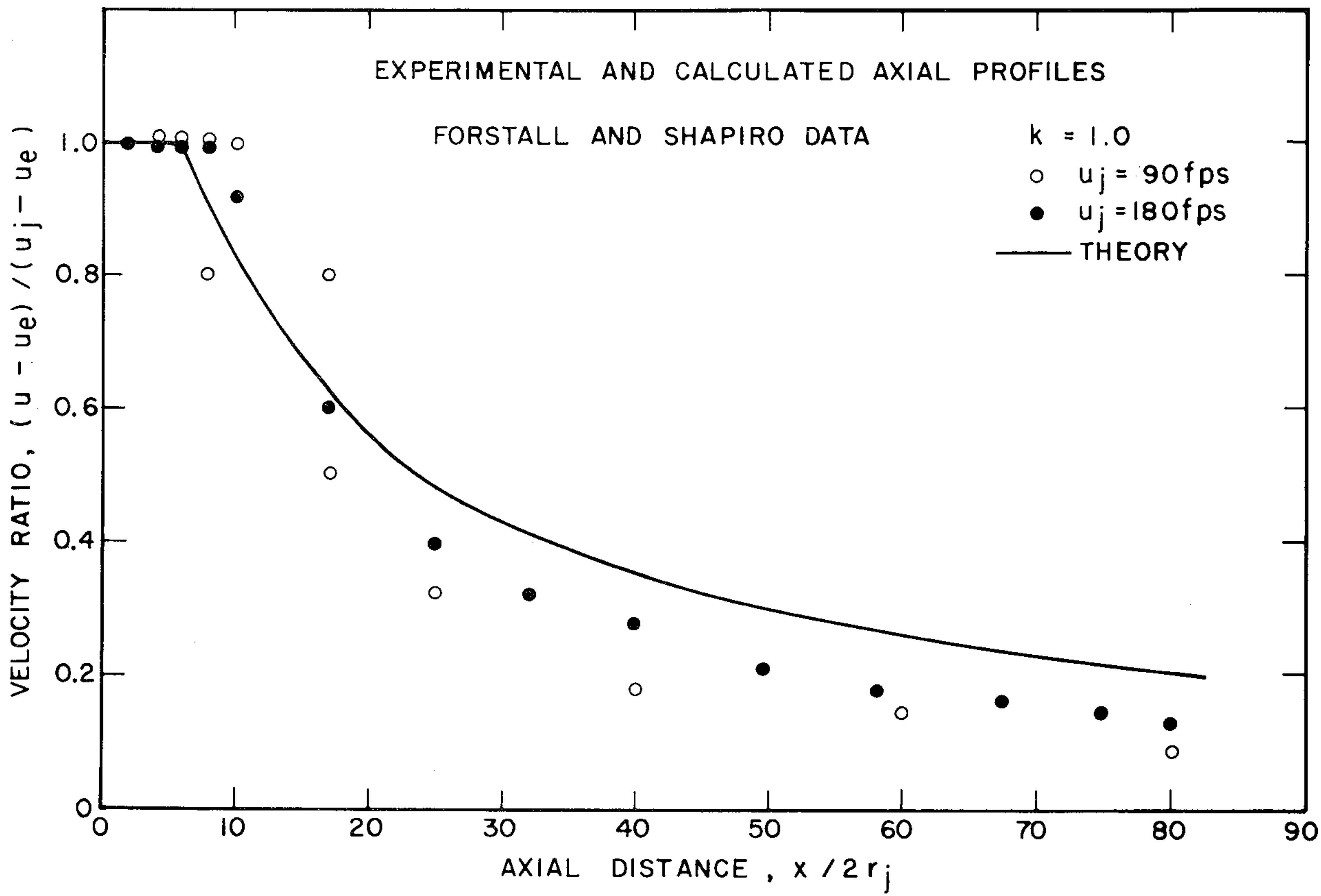
EXPERIMENTAL AND CALCULATED AXIAL PROFILES
FORSTALL AND SHAPIRO DATA
k = 1.0
uj = 90fps
uj = 180fps
THEORY
VELOCITY RATIO, (u - ue) / (uj - ue)
AXIAL DISTANCE , x / 2 rj
0
0.2
0.4
0.6
0.8
1.0
10
20
30
40
50
60
70
80
90

Figure 4

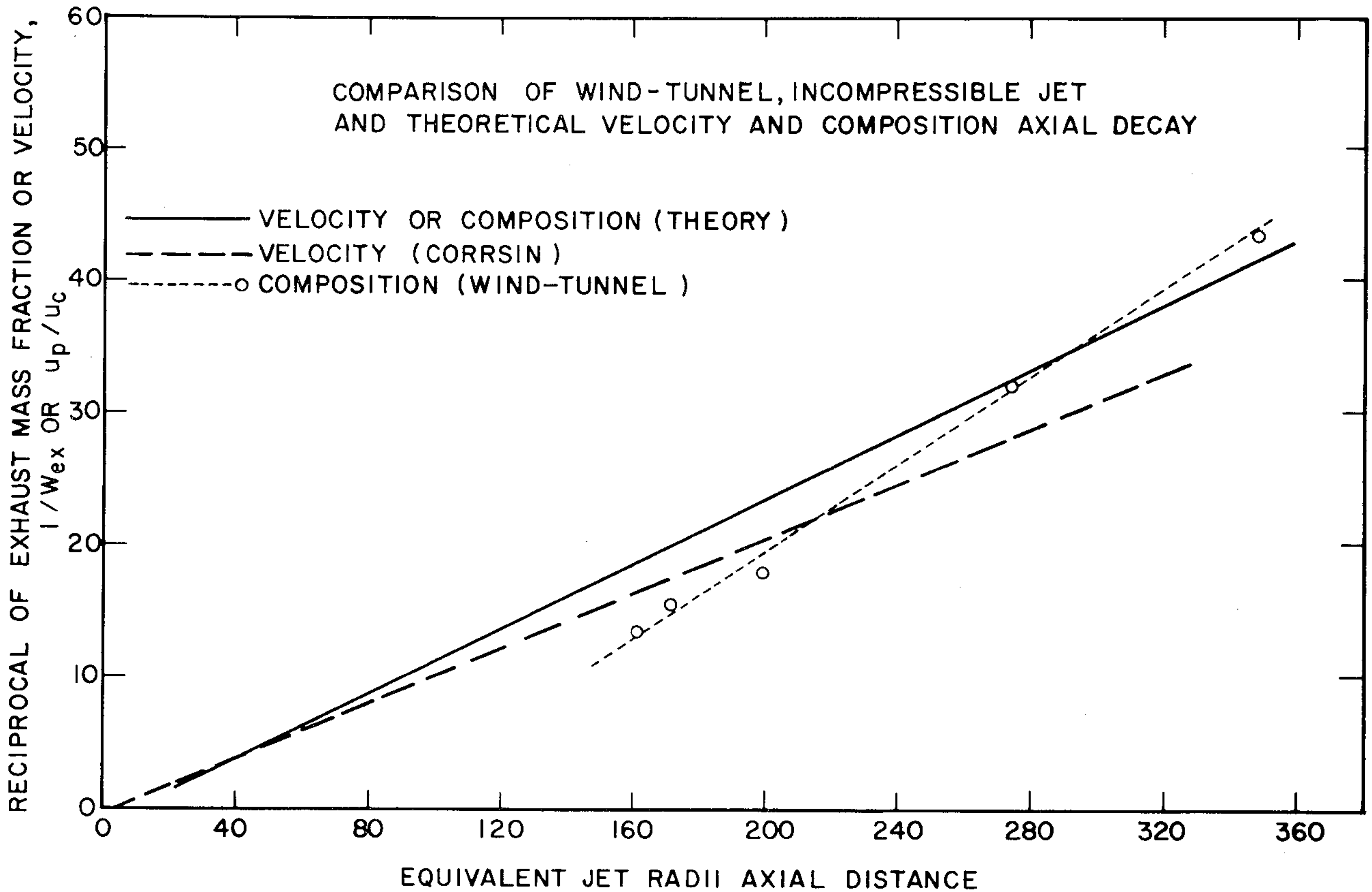
COMPARISON OF WIND-TUNNEL, INCOMPRESSIBLE JET
AND THEORETICAL VELOCITY AND COMPOSITION AXIAL DECAY
VELOCITY OR COMPOSITION (THEORY)
VELOCITY (CORRSIN)
COMPOSITION (WIND-TUNNEL)
RECIPROCAL OF EXHAUST MASS FRACTION OR VELOCITY,
$1/W_{ex}$ OR u_p/u_c
EQUIVALENT JET RADII AXIAL DISTANCE
0
10
20
30
40
50
60
0
40
80
120
160
200
240
280
320
360

Figure 5

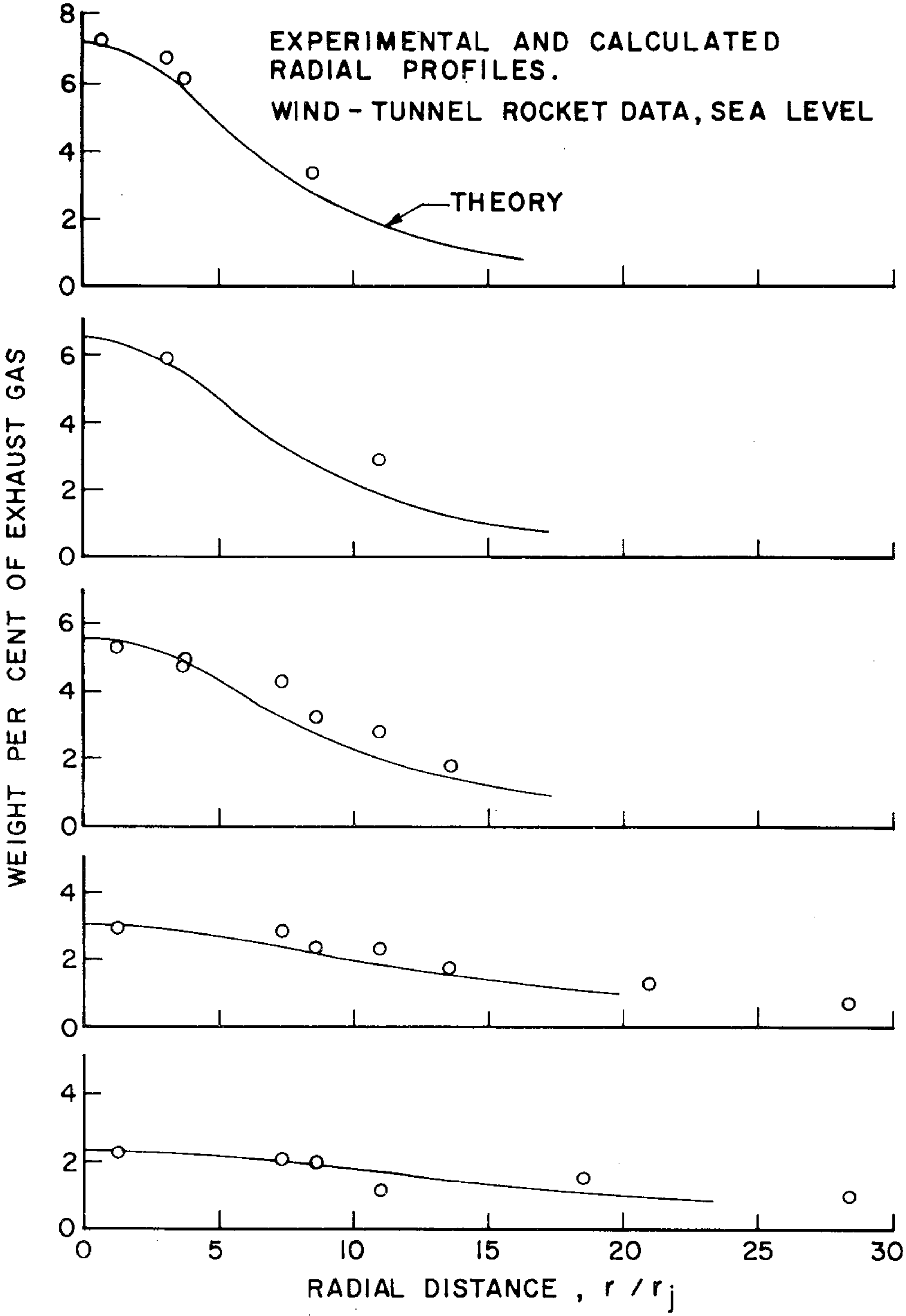

EXPERIMENTAL AND CALCULATED RADIAL PROFILES.
WIND-TUNNEL ROCKET DATA, SEA LEVEL
THEORY
WEIGHT PER CENT OF EXHAUST GAS
RADIAL DISTANCE , r / r_j
0
2
4
6
8
5
10
15
20
25
30

Figure 6

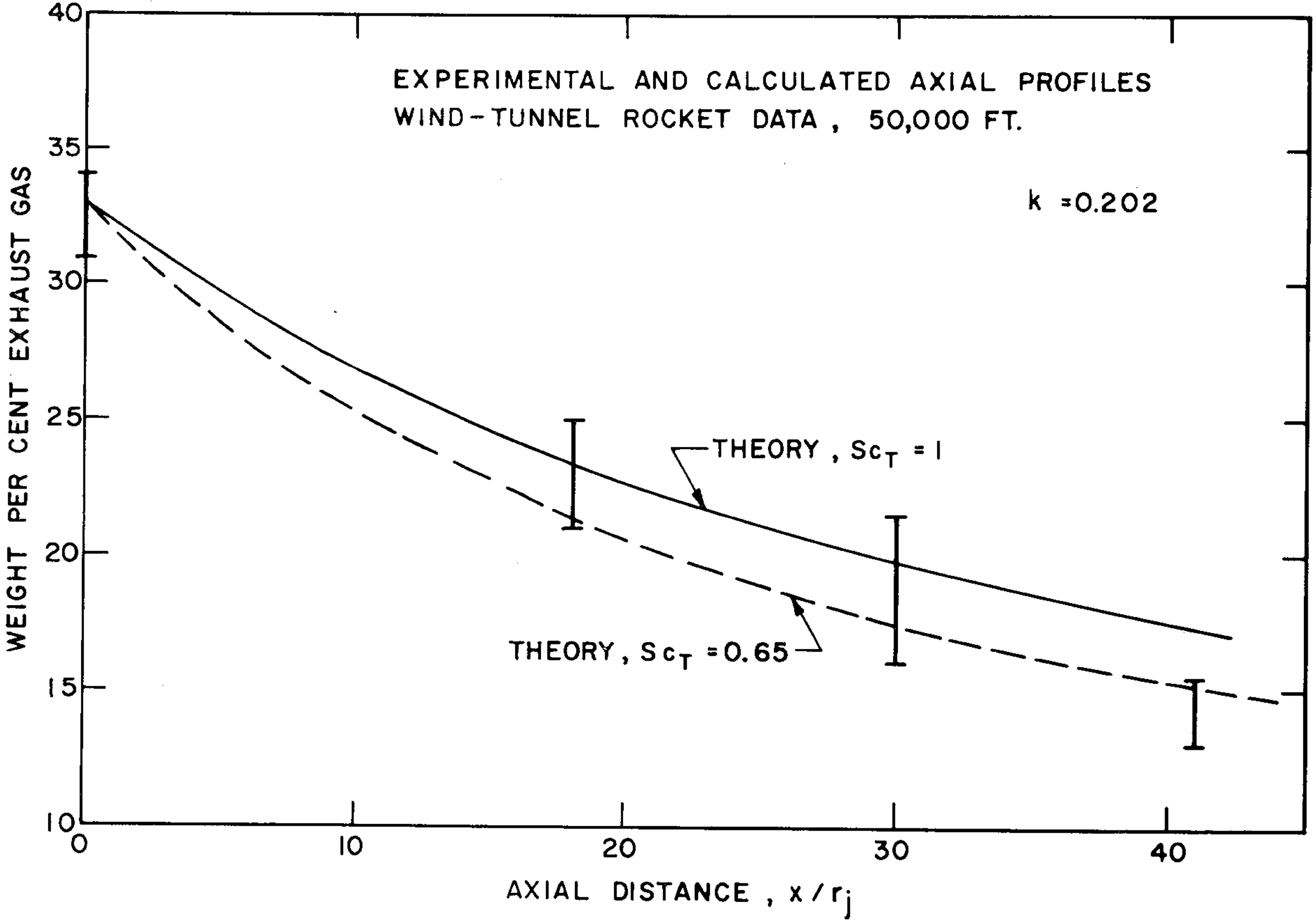
EXPERIMENTAL AND CALCULATED AXIAL PROFILES
WIND-TUNNEL ROCKET DATA, 50,000 FT.
k =0.202
THEORY, Sc_T = 1
THEORY, Sc_T =0.65
WEIGHT PER CENT EXHAUST GAS
AXIAL DISTANCE, x/r_j
40
35
30
25
20
15
10
0
10
20
30
40

Figure 7

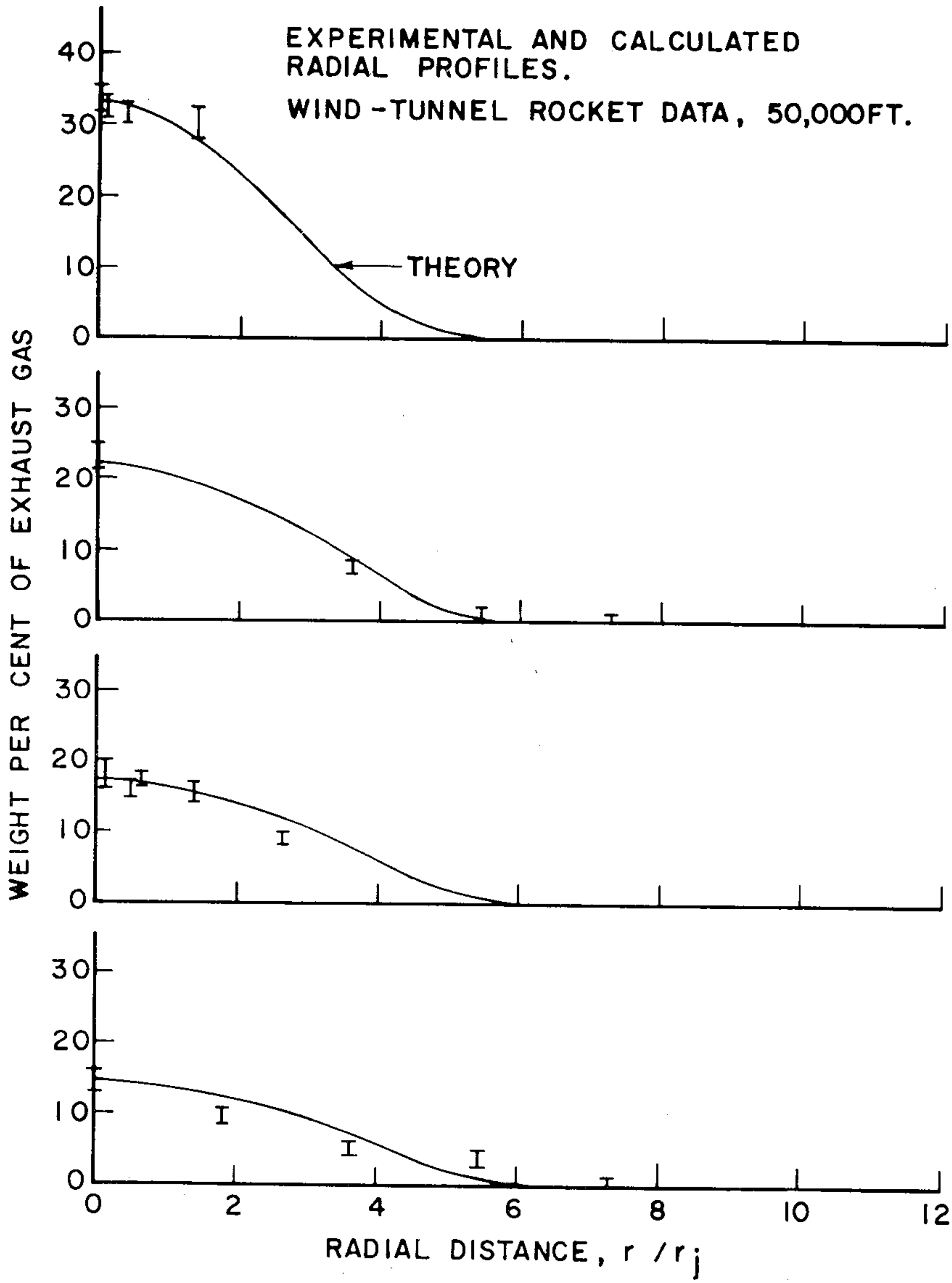

EXPERIMENTAL AND CALCULATED RADIAL PROFILES.
WIND-TUNNEL ROCKET DATA, 50,000FT.
THEORY
WEIGHT PER CENT OF EXHAUST GAS
RADIAL DISTANCE, r / r_j

Figure 8

REFERENCES

1. J. A. L. Thomson, "Launch Phase Radiation Studies: Appendix G, Some Elementary Consideration Concerning the Aerodynamic Structure of the Exhaust Plume at High Altitudes," General Dynamics/Convair Report ZPh-035, June 1959.
2. P. A. Libby, "Theoretical Analysis of Turbulent Mixing of Reactive Gases with Application to Supersonic Combustion of Hydrogen," ARS J. 32, 388-96 (1962).
3. J. O. Hinze, Turbulence (McGraw-Hill Book Company, New York, 1959), Chapter 6.
4. L. Howarth, "Concerning the Effect of Compressibility on Laminar Boundary Layers and Their Separation," Proc. Roy. Soc. (London) 194, 16-42 (1948).
5. A. A. Dorodnitsyn, "Laminar Boundary Layer in Compressible Fluid," Dokl. Akad. Nauk SSSR 34, 213-19 (1942).
6. F. P. Boynton, "Self-Preservation in Fully Expanded, Round Turbulent Jets," AIAA J. 1, 2176-78 (1963).
7. M. Thring and P. Newby, "Combustion Length of Enclosed Turbulent Flames," Fourth Symposium (International) on Combustion (Williams and Wilkins Co., Baltimore, 1953), pp. 789-96.
8. L. Ting and P. A. Libby, "Remarks on the Eddy Viscosity in Compressible Mixing Flows," J. Aerospace Sci. 27, 797-98 (1960).
9. H. S. Ribner, "The Generation of Sound by Turbulent Jets," Advances in Applied Mechanics, Vol. 8 (Academic Press, New York, 1964), pp. 103-182.
10. O. M. Phillips, "On the Generation of Sound by Turbulent Shear Layers," J. Fluid Mech. 9, 1-28 (1960).
11. J. C. Laurence, "Intensity, Scale, and Spectra of Turbulence in Mixing Region of Free Subsonic Jet," NASA Report 1292 (1956).

12. H. S. Carslaw and J. C. Jaeger, Conduction of Heat in Solids, 2nd Ed. (Clarendon Press, Oxford, 1959), p. 260.

13. J. I. Masters, "Some Applications in Physics of the P Function," J. Chem. Phys. 23, 1865-74 (1955).

14. F. P. Boynton and J. T. Neu, "Calculations of Adiabatic Flame Temperature of Afterburning Rocket Exhausts," General Dynamics/Astronautics Report ERR-AN-011, April 1960.

15. F. P. Boynton, "Chemical Equilibrium in Multicomponent Polyphase Systems," J. Chem. Phys. 32, 1880-81 (1960).

16. P. A. Libby, P. O. Baronti, and L. Napolitano, "Study of the Incompressible Turbulent Boundary Layer with Pressure Gradient," AIAA J. 2, 445-52 (1964).

17. H. Schlichting, Boundary Layer Theory, 4th Ed. (McGraw-Hill Book Company, New York, 1962), pp. 598-600.

18. S. Corrsin and M. S. Uberoi, "Further Experiments on the Flow and Heat Transfer in a Heated Turbulent Air Jet," NACA Report 998 (1950).

19. W. Forstall, Jr., and A. H. Shapiro, "Momentum and Mass Transfer in Coaxial Gas Jets," J. Appl. Mech. 17, 399-408 (1950).

20. J. M. Bowyer, Jr., et.al., General Dynamics/Astronautics Report No. ZR-AP-061-24, April 1962.